Simultaneous Frequency and Voltage Regulation with Static VAR Compensation

A Thesis

Presented in Partial Fulfilment of the Requirements for the

Degree of Master of Science

with a

Major in Electrical Engineering

in the

College of Graduate Studies

University of Idaho

by

Kendall Bean

Approved by:

Major Professor: Dakota Roberson, Ph.D.

Committee Members: Robert Borrelli, Ph.D.; Brian Johnson, Ph.D.

Department Administrator: Joseph Law, Ph.D.

May 2022

Abstract

Renewable energy sources (RES) are becoming increasingly prevalent in modern power systems. This increased penetration of RES helps to reduce carbon emissions due to power generation, but the nature of wind and solar electricity generation creates some unique problems from a power system stability perspective. Frequency stability in particular is a difficult aspect to maintain in a system with a high penetration of renewables. This is in part due to their lack of generator inertia and inability to alter generation on demand, requiring external power electronic devices to regulate the flow of power they produce to be in line with the stability needs of the system. As the world moves ever onward towards net-zero carbon emissions from power generation, new technologies or new applications of existing technologies will be needed to maintain a secure and stable power grid.

In this thesis, it is shown that a modest static VAR compensator (SVC) bank can effectively damp frequency oscillations caused by a misbehaving wind park due to load fluctuations. By using a phasor measurement unit (PMU) to track frequency and applying principles of Bode loop shaping, a frequency compensator is designed that allows the SVC to achieve this frequency damping while maintaining its ability to regulate voltage, the most common use case for SVCs, at the same time. By identifying frequencies where the system experiences oscillations using non-parametric broadband power spectral density (PSD) estimation and designing the compensator around them, these common power electronic devices, SVCs and PMUs, can be used to add a great deal of frequency stability to systems that traditionally struggle with frequency control, specifically RES such as wind parks that are rapidly increasing in prevalence in modern power grids.

Acknowledgements

I would like to thank Dr. Dakota Roberson, who strove to maintain meaningful contact throughout unpredictable conditions when it comes to helping his students. The onset of Covid-19 among other events made that job much harder, but he continued to provide invaluable support to his students regardless.

Dr. Brian Johnson provided great feedback and information sources for many topics as we worked on the project upon which this thesis is based for months on end.

Dr. Michael Haney's classes, while not always directly related to my work with control systems, introduced me into the wide world of modern infrastructure and cyber security, both of which are very germane to the modern conversations surrounding control systems.

Dedication

This thesis, and all the work I do, is dedicated to my wife and family. Amberly has sacrificed as much as if not more than I have for me finish my degree. She and my son Gabriel are the reason I seek to improve myself every day.

Table of Contents

List of Figures

Chapter 1: Introduction

The summer of 1996 was particularly hot in the Northwestern United States, with daily temperatures frequently averaging over 100 degrees Fahrenheit. This led to higher demands than what had been historically necessary or what operators in the Western Systems Coordinating Council (WSCC, later renamed to the Western Electricity Coordinating Council, WECC) had projected; maintenance and upgrades were also underway at the time [1], meaning that generators, transformers, relays, and entire sections of transmission lines were down. This meant higher stress on the equipment and lines that were operating, and less available spinning reserves. As any individual transmission line transfers more and more power, it heats up and begins to sag, even if it is still within its operational limits.

On July 2, a combination of poor transmission line maintenance, human misoperation, degraded or faulty protective equipment, and scheduled out-of-service equipment unavailability caused cascading blackouts to occur when two 345 kV lines faulted for unrelated reasons [1]. One arced-to-tree while the other was opened due to a misconfigured and degraded protective relay. Unseasonably high power demand due to the weather and high electricity transfer from plants in Canada due to ideal generation conditions resulted in power transfer at levels with insufficient safety margins. This ultimately led to what might have otherwise been minor to moderate line faults becoming system-wide cascading blackouts in a remarkably short time frame. The initial faults occurred at 14:24.37 MDT, and within 33 seconds, the WSCC had been split into 5 separate electrical islands through automated relay opening, generator cutoffs, and load shedding.

A similar sequence of events happen again the very next day, July 3, 1996 [1]. In the heat of the day, at 14:03 MDT, a line arced to a tree and the selfsame faulty protective device disconnected a second line again. Fortunately, many lines were forcibly restricted in their allowed power transmission as the previous days events were investigated. This

meant that automated voltage protection did not trip as fast, and the lines were not running as hot, meaning they did not sag as much and were in less danger of arcing or blowing out from the sudden increase in transmission across them. The July 3 faults therefore still resulted in blackouts, but they were manually controlled blackouts that affected smaller areas, and happened over a matter of minutes, as opposed to seconds. There were no islanding events on July 3, 1996, and power was restored to virtually all customers within an hour.

Still considering the necessary changes in operating procedures and transmission requirements illustrated by the July 2-3 blackouts, it was not long until another major outage occurred in the WSCC. On August 10, 1996 along the California-Oregon Intertie (COI), three different lightly loaded 500 kV transmission lines faulted [1]. Two arced to trees and faulted to ground, while one had a circuit breaker its and associated transformer that were out of service. These faults occurred at least 45 minutes apart from each other. Individually, these lines did not account for much of the power flow through the intertie, but in aggregate, they provided significant reactive power support to the larger transmission lines along the COI. The Keeler circuit breaker and transformer that were out of commission had an SVC on the low side of the 500 kV/230 kV transformer, which could have aided the reactive power deficit the system faced after the three faults, though it is unlikely it would have prevented the blackouts entirely. Once these three transmission lines had been opened, voltage levels along the west coast, especially in Northern California, began to drop.

Due to the recent blackouts that were caused in large part by transferring too much power along lines without enough of a safety margin, by August 10 the power transfer limits along the COI had been set lower than they were on July 2 [1]. This meant that the dropping of these three lines did not result in widespread and near immediate blackouts. However, the loading on the remaining lines was still high, due to both the dropped lines and several instances of planned out-of-service transformers and lines, including an SVC.

As voltage levels dropped, voltage and power oscillations began to occur in the system. Over an hour an a half after the first line flashed to a tree, the McNary generators tripped offline, which caused the WSCC to split into four islands in just two and a half minutes, with a fifth island separating off in another four minutes.

Several conclusions were eventually reached by the NERC Disturbance Analysis Working Group for both the July 2-3 incidents and the August 10 incident. The report in [1] states that while many conclusions were made, some primary causes were of particular interest. In the July 2 incident, it was determined that the primary cause of the blackouts was insufficient voltage support for the amount of power transferred through the Northwest transmission lines. Additionally, they determined that many of the automated responses ended up harming the system as a whole, and that wide-area monitoring would be necessary to ensure that events such as voltage collapse do not spread to the rest of the system. The effects of the overburdened transmission lines in the face of significant and simultaneous transient events were immediate and dramatic.

The cause of the August 10 incident was different in a few crucial ways. Voltage demand was still high on the system, but power transmission through the lines was more strictly rationed following the July 2-3 blackouts [1]. Additionally, the faults happened relatively gradually. Once some of the McNary protective relays tripped, other generators began to try to compensate for the removed generation. Despite the other generators attempting to make up for lost active power generation, the dropped lines and reduced number of generators caused there to be insufficient reactive power in the grid. This caused the 0.25 Hz inter-area mode to become negatively damped [2], causing all three COI lines to open in slightly over a minute of each other. The resulting swings in generation and demand caused further blackouts within the newly created electrical islands.

Even though lessons were learned from the 1996 blackouts regarding frequency oscillations within highly loaded power grids, the push for increased RES generation is

making frequency control problems even more prevalent in modern power grids [3–6]. Specifically, the increased emphasis on RES such as wind and solar energy is decreasing the amount of spinning reserve many grids have. The lower system inertia means that small deviations in frequency are harder to correct for, and the complex control systems necessary to connect asynchronous generation sources such as wind farms to the grid create the possibility for additional dynamics to manifest and cause problems, such as subsynchronous control interactions (SSCI). A relatively recent case of RES vulnerability to frequency instability can be seen in the September 28, 2016 blackouts that happened across Southern Australia.

On September 28, 2016, at approximately 16:16 ACST, two tornadoes nearly simultaneously damaged three transmission lines, causing them to go offline and initiating a sequence of faults that resulted in voltage dips [7]. Protective features of nine wind farms began tripping, and over the course of the next two minutes, the power output of these wind farms dropped dramatically. This forced more power to come in from other sources, which in turn tripped more lines and ended up islanding the Southern Australian (SA) grid by 16:18. The sudden disparity of load versus generation in the newly islanded area caused major frequency oscillations, ultimately blacking out the SA grid.

The final report on this event, [7], states that one of the nine wind farms had a control setting that caused it to trip prematurely, and further degrade the rest of the system from that lack of generation. The other eight wind farms successfully rode through the disturbance, and their simulations indicated that if the faulty farm had not tripped offline completely but had instead reduced its generation like the other eight, then the blackout would have been prevented. Even with that conclusion, they still acknowledged and suggested the need for remedial actions addressing the lack of inertia in the SA grid. They also recommended non-generation control devices be made available to stabilize frequency deviations over the long term, as wind generators are largely unable to correct for frequency deviations on their own.

The function of the proposed SVC based frequency regulator is very germane to both the August 10, 1996 Western Interconnect blackouts and the September 28, 2016 Southern Australia blackouts, but can also be utilized for any small signal instabilities in power systems. There are two key factors regarding the frequency oscillations in the August 10, 1996 Western Interconnect incident: they were gradual, meaning there was time for appropriate protective equipment to implement remedial actions; and they were due in large part to a lack of reactive power control. The report [1] states that the generators seeking to make up for the McNary generators tripping were controlled for power factor, not voltage levels, which follow reactive power. In the 2016 Southern Australia incident, the lack of system inertia and inability to compensate for frequency deviations inherent in the induction generators of wind farms led to a fragile system that quickly fell to simultaneous faults.

In this thesis, a control scheme utilizing an SVC for Voltage-based Frequency Control (VFC) and a PMU as its sensor will be described and demonstrated on a modified version of the IEEE 12-bus system with a 166.7 MVA wind park attached. The scheme will be shown to provide good damping for load fluctuations that would otherwise cause the wind park to generate substantial sustained power oscillations. Such control schemes could prevent costly and dangerous outages in the future by simultaneously controlling for voltage level (reactive power support) and frequency, utilizing already widely used power system components and wide-area sensors.

Chapter 2: Literature Review

A review of the literature surrounding the damping of small signal oscillations reveals that grid frequency stability, especially for wide area systems, is a pressing issue with many ways to approach it. It is helpful to look at various devices and their applications in power system frequency stability.

Small-signal frequency oscillations and how to compensate for them have been the subject of many studies. The most common form of frequency control is a power system stabilizer (PSS), which operates on the principle of modulating generator excitation to generate electrical torque in phase with rotor speed deviations to damp generator rotor oscillations [8]. This reliance on generator dynamics means that turbines not generating synchronously with the grid, such as wind farms, require special considerations when trying to implement a PSS [9, 10], and they are not usually considered standard in wind turbines. The very narrow applicability of standard PSS configurations to RES means they do not make a good candidate as the basis for control schemes focused on RES frequency compensation. Even in general cases, SVCs and other FACTS devices provide superior stability margins to traditional PSS [11].

PMUs can be used as the sensors for traditional frequency controls, but do not make ideal sensors for higher frequency processes, as investigated by [12]. The authors of [12] simulated a single-machine infinite-bus (SMIB) system with a PSS attached to observe the effect of changing from an analog input, simulated as a 1000 Hz sampling rate, to that of a PMU with a reporting rate of 50 or 60 Hz. There were noticeable performance differences between a simulated "ideal" PMU that did not account for estimation errors, leakage effects, and sampling issues, as compared to the more realistically simulated PMU that did account for those properties. The "ideal" simulated PMU performed better, but both served as adequate sensors for a PSS for frequencies below 20 Hz, with distinct errors and deviations occurring at 50 Hz and above. This agrees with the standard controls

engineering understanding of cut-off or Nyquist frequencies, where a sensor becomes ineffective at frequencies past half its reporting rate.

A thesis written in 2004 presents a very similar frequency control scheme to what is proposed in this thesis. Reference [13] uses PMUs as sensors for a wide area small-signal stability controller, taking signal samples shortly after small disturbances have been cleared to actively monitor for growing inter-area modes, also using SVCs to damp any detected modes. The primary differences between the scheme presented in [13] and the one presented in this paper are:

- Their scheme spends processing power on identifying and actively monitoring modes;
- Their scheme switches SVCs over from voltage regulation to full time frequency regulation when a mode is detected to be oscillating

The proposed scheme identifies primary modes before hand to reduce the processing power needed and the resulting potential signal delay, as well as controlling the SVCs to regulate for voltage and frequency simultaneously. The theory behind both control schemes is very similar, with theirs using an active system shape estimation algorithm and the present scheme utilizing a generalized identification of system stability margins via non-parametric broadband power estimation to design filter parameters before implementing the controller.

The paper in [14] gives a detailed outline of how using a PMU impacts the closed-loop transfer function of a controller and how time delay impacts the performance of a controller. They propose a protective control scheme dubbed an "excessive regeneration detector" or ERD that uses variable loop gain to dynamically alter the feedback gain on their controller and damp oscillations past a certain threshold. They did not simulate real hardware in that study, and used an established, well identified model for testing, namely the miniWECC model of the North American Power System. The proposed SVC frequency compensator builds on the concept of reducing time delay in the control signal

as well as shaping a transfer function based on PMU dynamics. Unlike the paper in [14], this is done while adapting the control method to fit to real hardware in an SVC, as well as describing a general use system identification method that can be used to design the transfer function. Many of the principles of Bode loop shaping used in [14] are also used in the design of the compensator developed.

The authors of [15] propose a wide-area, PMU based control scheme to detect the difference between the different portions of the California-Oregon Intertie to give active power injection commands to strategically located sites along the intertie in order to damp known oscillatory modes in the COI. They design a filter and saturation limit for their detection scheme to guide its control actions to focus only on low frequency 0.2 Hz to 1.0 Hz modes. The controller successfully attenuates the 0.25 Hz mode oscillations after a simulated disturbance along the North-South corridor of the COI. Reference [15] also provides a supervisory system to monitor the controller and disconnect it from the system if any number of safety conditions are triggered. The overall result is a robust system that effectively damps inter-area modes present in the WECC and a functioning hardware prototype, but its design is such that it is very specific to the WECC. It relied on the many years of study that have gone in to characterizing the dynamics of low frequency oscillations within the WECC.

The authors of [16] propose a decentralized sliding mode control (SMC) scheme to augment standard proportional-integral (PI) control of both frequency and voltage on a wide-area system. It is a nonlinear control scheme that uses separate control laws for both the frequency and voltage regulation. The frequency regulation is achieved via direct control of generator steam valves, adjusting steam output and thereby generator rotational frequency directly according to the law given. This frequency control law also takes tie line power transfer levels into account so as to ensure adequate power remains available while frequency is regulated. Voltage control is achieved through an SMC augmenting standard SVC control parameters. However, the authors of [16] con-

trolled voltage and frequency separately, whereas the proposed compensator of this thesis controls frequency directly through reactive power modulation provided by SVCs, while simultaneously maintaining their ability to regulate voltage. It should also be noted that they do not mention what they used for a sensor, instead implying that they did not simulate sensor hardware in their MATLAB simulation.

Reference [17] seeks to use a strict Lyapunov energy function (SLEF) as a nonlinear external control loop for the purpose of VFC. They model the SVCs and loads as ODEs with the load represented as "a voltage dependent function with an unknown parameter [17]." This mathematical model is able to function as a control law with unknown parameters in the load model, including having an unknown time derivative of the reference signal. However, in order to construct an SLEF while preserving the complete topology of the power system, constant active power must be assumed. Their feedback loop relies on local variables within the SVC, and there are five significant tuning variables. Because of this highly self-contained control loop, they are able to use the SVC's PLL as their primary sensor. However, this does nothing to synchronize various distributed SVCs on a power system to work in tandem, and indeed without using a synchrophasor device, there would be no way for distributed SVCs to coordinate measurements using only their internal PLLs. [17] presents a robust nonlinear control scheme that focuses on practical systems via a lack of defined load variables, but relies on several mathematical assumptions about the system model that may not always be applicable, in addition to the complexity of the mathematical basis of the model itself.

In [18], the authors use a supplemental control loop on SVCs for the purpose of VFC, utilizing droop (lag) and PI transfer functions for their control scheme. Their focus, similar to that of the SVC frequency compensator developed here, is to use local measurements and conventional controllers to increase power system frequency stability. Their approach does differ mathematically from the approach taken in this paper, focusing on changing bus voltage magnitudes in order to regulate active power consumption.

They use frequency deviation as an input signal, as does the presently developed frequency regulator. Their use of a PI control scheme requires several other filters to reduce noise sensitivity and ensure that it does not interfere with the standard voltage regulating functions of the SVC. Additionally, they use a PLL for their frequency measurements, just as [17] does. This limits the ability to scale this type of control scheme to larger areas due to the lack of geosynchronous measurements. The approach in [18] is overall much more mathematically straightforward than in [17], and can improve frequency control without disturbing the improved voltage response that SVCs are most commonly implemented for.

The authors of [6] use a synchronous condenser, which is a synchronous machine that does not consume or produce electricity beyond internal losses, but rather serves to provide or absorb reactive power to the grid, as the primary actuator for a 2-band controller that damps low frequency oscillations. The filters for their controllers need to be tuned for local modes, and they use four well known grid models for their testing. They also make use of a proprietary device called a Multi-functional Multi-band Power System Stabilizer, or MF-MBPSS, to filter multiple frequency signals into one output command. Their control approach is to have the synchronous condenser acting as a form of virtual inertia. The performance of their control scheme was good for all of their tested systems, but the reliance on proprietary devices and use of already well defined systems as test systems limits the general applicability of their findings.

Other FACTS devices are also able to regulate frequency through the rapid control of reactive power. One such device that has seen an increase in usage recently is the static synchronous compensator, or STATCOM, which has largely the same functionality as an SVC but operates on entirely different principles than an SVC, relying on solid state electronic switching converters rather than external reactors and capacitor banks [19]. They are also more expensive and less common than standard SVC devices [20,21]. They have been shown in [22] to have superior damping capabilities frequency oscillations

caused by a fault for a doubly-fed induction generator (DFIG) based wind farm. Series and shunt compensation can be used in tandem, as shown in [23]. The authors use a thyristor-controlled series compensator (TCSC) together with a STATCOM to damp disturbances due to both line outages and excitation system misoperations. They present both layered single-input, single-output (SISO) control schemes and connected multi-input, multi-output (MIMO) schemes for the combination of FACTS devices.

Acknowledging the work done investigating more advanced and higher performance FACTS devices, the wider applicability of SVCs compared to most other FACTS devices gives cause for this study to focus on using SVCs as the primary actuator.

Chapter 3: Control Design

3.1 General Principles of Power Grid Operation

The electric power grid operates on two major principles [24]:

- Maintain constant balance between generator and load; and
- Maintain constant uptime by adjusting power flow to meet equipment specifications.

These principles encompass both the economic and functional motivations for maintaining the grid. There are two major parameters that characterize whether or not the power grid is successfully meeting these operating principles: voltage and frequency [25]. Both voltage and frequency must be regulated to maintain a stable operational state at predetermined levels for the grid to be considered operating normally.

3.1.1 Stability

In power system contexts, stability can be broadly categorized as either steady-state stability or transient stability. In general, steady state stability refers to a power system's ability to maintain stable operation under a fixed set of conditions, including constant generation and load, for a long period of time [8, 26]. Transient stability refers to a system's ability to remain operable throughout of large but short deviation from nominal operating conditions, and then return to some stable, if not necessarily nominal, operating point. In most contexts, stability in AC power systems refers to the voltage or power angle of the power being produced by generators throughout the system, denoted as "angle stability."

When a system has angle stability, it can also be said to have frequency stability, as the angle between peak voltage values corresponds directly with the physical spinning of

generators. If all generators are spinning at the same speed, i.e. at the same frequency, it creates a steady-state frequency stable system. Part of this steady-state frequency stability is the coupling of the generators in the system. When one generator has a voltage angle that is ahead of the rest of the system, it must generate additional power to maintain this lead, which acts as a slowing force on the generator. Similarly, when a generator has a voltage angle that is lagging the synchronous signal on the grid, it is not providing as much power, which removes some the force acting on the generator, allowing it to speed up [26].

Transient stability, sometimes referred to as "dynamic stability," can be analyzed as a function of the magnitude of the transient disturbance and the time duration of the disturbance. There exists a critical point of the combined magnitude and duration of a disturbance past which a system cannot recover. This point defines the transient stability margins of that system. For example, a breaker reclosing can suddenly disconnect and then reconnect a generator to the power grid [26]. The lack of load would cause the generator to have nothing to electromagnetically push against and it would begin to accelerate its rotational speed. Past a certain duration, the generator would have built up too much speed to be able to safely dissipate its excess kinetic energy upon reconnecting to the grid.

Related to these two types of angle, or frequency, stability is "voltage stability." As the load on a power system increases, the power consumption increases, but only up to a point [26]. Beyond that, voltage levels cannot be maintained unless reactive power compensation is provided to regulate, or "support," the voltage magnitude. Voltage instability occurs when loads try to draw too much power or generators/transmission lines are unable to deliver enough power, and the resulting oscillations as system controllers try to adjust for the imbalance can cause devices to trip offline, causing voltage collapse. Voltage and frequency stability can have significant effect on one other, both in how disturbances affect the system and how those disturbances are compensated for.

Many types of disturbances have both a transient and steady-state effect on power transmission. A line grounding to a tree and faulting would suddenly change the power and reactive power transmitted across nearby remaining lines, which would cause a transient effect on connected generators. Until the line is repaired, the reduced transmission capacity could cause generators to have to work harder to generate sufficient power to supply connected loads, as well as increase the current on the remaining lines, creating a steady-state disturbance to the system as well.

3.1.2 Regulation

Grid stability is achieved through regulatory devices that actively or passively help maintain voltage and frequency levels on the grid at predefined points. Control schemes for both parameters vary from near omnipresent to purely theoretical, and from simple monofunction devices to complex wide area considerations. There are three basic categories of control [3]:

- Primary controls - Operates on a time scale of seconds after a disturbance occurs, serves to prevent the system from becoming permanently damaged or collapsing; they are responsible for damping transient oscillations.

- Secondary controls - Operates on a time scale of seconds to minutes, serves to restore the system back to its original steady-state operating point; they are responsible for maintaining steady-state stability.

- Tertiary controls - Operates on a time scale of minutes to hours, serves to slowly disengage the secondary control mechanisms and re-establish generation/load balance; they are a primarily economic consideration that also free up the secondary controls for further control actions.

A basic understanding of the most common devices and methods used for frequency and voltage control will provide a backdrop helpful for understanding the place of the

proposed SVC frequency regulator in the larger picture of electric power regulation.

When load changes on a system, the electrical torque on the generators changes with it, resulting in a mismatch between the electrical torque and mechanical torque of a turbine shaft. This results in changes to generator speed that exhibits as oscillatory motion as physical forces conserve the balance between potential and kinetic energy [8,26]. A turbine governor acts as a control mechanism that changes the amount of force being applied to turbine, for example via a steam valve, to adjust its rotational speed in response to system disturbances. In large systems, governors have control schemes to help reduce the conflict between individual governors trying to control the frequency of the entire system through their respective generators [3, 8]. Governors act as primary controllers that stop frequency deviations from becoming worse once the threshold for control action is reached [3].

Once the frequency is no longer changing, automatic generation control (AGC) will activate to try and restore the system to its original operating frequency [3,8]. There are various implementations of AGC [3]. Smaller grids might use constant frequency control, which adjusts plant power output based only on frequency deviations. This ensures the most efficient use of energy, but would cause too much conflict between controllers on a larger grid. Constant net interchange control only looks at the flow at grid interchanges and not at frequency deviations, which can be helpful if a section of grid loses major generators and cannot effectively control frequency on their own. For large interconnected grids, tie-line bias control places responsibility for frequency restoration on the section of grid that experienced the disturbance. This both minimizes the economic impact on other grid operators and leaves the operators with the most information in charge of bringing frequency back to nominal safely. AGC in all its forms acts as a secondary controller for system frequency.

Voltage regulation is accomplished through controlling reactive power in a system [8]. Generators use automatic voltage regulators (AVRs) to control field excitation within

the turbines as a means of primary control. Secondary control throughout the system is usually achieved by some combination of reactive power injection or absorption, line reactance compensation, and voltage regulation via transformers, especially tap changing transformers.

Permanent fixtures, such as shunt reactors or capacitors, can improve the reactive power on a system. Shunt capacitors are a very economical and common means of increasing reactive power along a transmission line, but the reactive power they provide is proportional to the square of the line voltage [8], so they are least effective where they are needed most. Shunt reactors are usually required for extra-high voltage (EHV) lines of significant length or with weak sources, limiting overvoltages when the line has an open circuit or is lightly loaded. They may need to be switched in and out depending on loading conditions.

A capacitor placed in series with line conductors will reduce the transfer reactance between two buses, which reduces the reactive power loss in the line. The reactive power produced by a series capacitor increases with the amount of power transferred across it, and is thereby at least partially self-regulating [8]. It reduces voltage drop in steady-state and responds near instantaneously to current, effectively improving flicker between the grid and a fluctuating load. A number of issues they experience with startup energization reduces their applicability in distribution systems, but transmission systems use them extensively for reactive power compensation. It is, however, undesirable for a line to have complete compensation, as that would increase the voltage angle sensitivity and create subsynchronous resonances. Even properly used, series capacitors can create a series-resonant circuit that has a natural electrical frequency the same as or close to the natural mechanical frequency of a nearby turbine shaft, which can also create subsynchronous resonance. All of the previously mentioned methods of voltage control, namely shunt reactors, shunt capacitors, and series capacitors, are installed directly onto transmission lines, making them less economically viable solutions for buses with multiple

intersecting lines.

While various transformer architectures exist for a variety of specialized needs, the type most commonly used for active voltage and reactive power regulation is the Under-Load Tap Changer (ULTC) transformer, sometimes referred to as an On-Load Tap Changer (OLTC) or simply as a Load Tap Changer (LTC) transformer. In all cases, the names serves to differentiate it from transformers than can only have their windings adjusted when disconnected from the system. LTC transformers can adjust their windings throughout the day to match changing load schedules during normal operation [8]. The transformer taps can control the reactive power flow between the secitons of the system it connects, thereby minimizing power losses and changing network voltage to be high during high loading, within line thermal limits, or minimal during light loading.

In addition to the previously mentioned methods, various forms of static VAR compensation can be used to generate or absorb reactive power for a greater degree and faster control of reactive power within a transmission system. SVCs are also used on distribution systems to prevent voltage flicker, but transmission systems are the focus of the present research. Though not exhaustive, a more thorough exploration into the relevant types of static VAR systems will be undertaken in Section 3.2.1.

Voltage and frequency control are traditionally assessed separately [8], but they are ultimately coupled and what affects one affects the other, if not always strongly [26, 27]. If voltage in a small grid section or an islanded grid decreases, the effective loading decreases as well, which also decreases the amount of effective power transfer out of the system. Voltage levels can be quickly changed along transmission systems to decrease loading as a form of primary control in emergency events, providing generators the time and ability to adjust frequency without needing to resort to automatic load shedding. The reduced voltage levels can be sustained for however long it takes for the generators to adjust frequency, and then slowly remove the voltage regulation once the system is prepared to return to normal operating level [27]. In this way, controlling voltage and

reactive power levels in a system can act as a vehicle through which to control frequency and provide greater frequency stability.

3.2 Summary of Significant Hardware

One of the primary goals of this research is to develop a method of damping small-signal frequency deviations using widely available, already installed power grid control technologies so as to minimize the potential costs associated with implementing the developed protection scheme. To that end, a PMU and an SVC are chosen as the sensor and actuator of the regulator design, respectively, in the test system used. They are readily available in many constrained power systems, and it is likely that their adoption will continue to increase as the penetration of RES steadily increases.

PMUs deliver measurements at higher fidelity and a higher sampling rate than many traditional SCADA-based measurement devices [28], and can synchronize measurements across large areas through GPS time-stamping, improving state estimation and protection alarms. SVCs are already present in a number of long distance transmission lines to support voltage stability and increase power factor through reactive power injection, and have been used. It is demonstrated that with minimal control assumptions regarding system configuration, these two devices can significantly increase the security of the power system by damping sustained oscillations. A brief description of how each device functions follows.

3.2.1 Static VAR Compensators

Static VAR compensators (SVCs) are power electronic devices that use controlled shunt (anti-parallel) thyristors to inject controlled lagging reactive power into a connected system. They comprise one of the devices that have been developed during implementation of Flexible AC Transmission Systems (FACTS), which enable previously built transmission systems to control their active and reactive power much faster than through

traditional generator-based controls [29].

Thyristor-Controlled Reactor

As explained in more detail in [30], a thyristor-controlled reactor (TCR) consists of a pair of oppositely oriented thyristors that are used to control current flow to a series connected reactor. One thyristor valve conducts in positive half-cycles and the other in negative half-cycles of the supply voltage. The controllable range of the thyristor firing angle, α, is from 90° to 180°, with 90° representing full thyristor conduction and continuous current flow that gradually reduces to discontinuous symmetrical current pulses as α increases to 180°, where the current flow ceases entirely. Once a thyristor valve is fired, it naturally turns off at the current zero crossing. Because the opposing thyristors operate on positive and negative voltage half-cycles respectively, each thyristor can only implement changes to firing angle on the next half-cycle.

This variable control of the current to the series reactor causes the TCR to act like a variable susceptance on the attached bus [30]. The fundamental current on the bus is proportional to this variable susceptance, and because the reactive power is in turn proportional to the bus current,the TCR can control the reactive power being provided or absorbed by the reactor. For firing angles greater than 90°, i.e. when the current to the reactor is being at all restricted, the current signal becomes non-sinusoidal and harmonics are introduced. If the thyristors are fired symmetrically, due to one operating on positive and one on negative half-cycles, only odd-ordered harmonics are produced. These harmonics are usually compensated for through filters. For a 3-phase TCR, three single-phase TCRs are delta connected to each other, with the reactors in series on either side of each anti-parallel thyristor pair to protect them from AC voltage surges should a short-circuit occur. The 3-phase configuration largely has the same operating dynamics as the single phase configuration, with some variations in the filtering for harmonics being necessary.

Thyristor-Switched Capacitor

Like a TCR, a thyristor-switched capacitor (TSC) has a pair of anti-parallel thyristors that are connected in series with a capacitor and a current limiting small reactor [30]. The thyristors are controlled to turn on when the the voltage across the thyristor valves is minimum in order to minimize the transient that occurs from switching a capacitor in and out of a circuit. The thyristors turn off when the current crosses zero, which corresponds to the supply voltage being at a peak. The small series reactor limits the current transient during overvoltages and when switching occurs at incorrect instants. Also similar to a TCR, a 3-phase TSC consists of three single-phase TSCs connected in delta. Practical TSC compensators use multiple shunt connected equivalent 3-phase TSC banks. TSCs include hysteresis elements in their control to prevent the frequent switching in and out, referred to as "chatter," of capacitors.

TSC-TCR Static VAR Compensator

A common configuration for a static VAR compensator is to connect one or more TSC devices in parallel with a TCR [30]. Each capacitor can be switched in or out individually, providing the continuous control of the TCR within each discrete reactive power step of the TSCs. The TSCs also help to reduce the harmonics generated by the TCR. Using TSCs as capacitive elements instead of standard mechanically switched capacitors (MSCs) provides greater flexibility to the system, specifically during large disturbances. TCRs with fixed capacitors tend to resonate with system impedance during large disturbances, especially when loads are dropped after severe voltage swings. A TSC-TCR SVC can quickly disconnect its capacitors to avoid this type of resonance. The capacitors in a TSC can also be switched in and out a virtually unlimited number of times, as opposed to MSCs.

The TSC-TCR configuration for an SVC is fairly common [29], though TCRs can

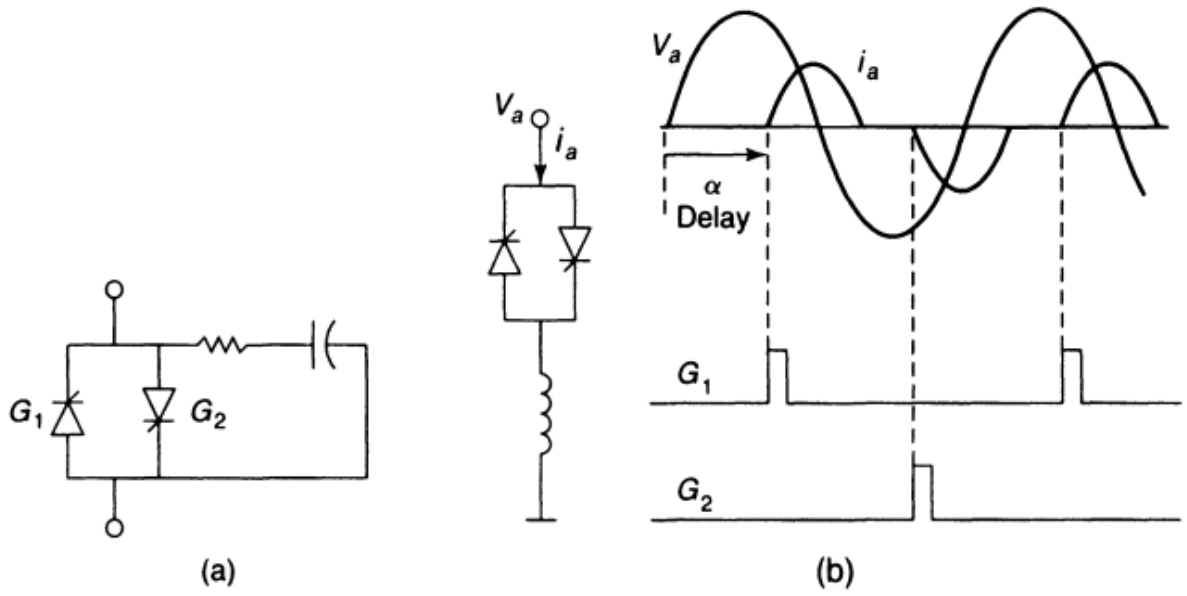

Figure 3.1: Illustration of (a) a switched reactor configuration and (b) a controlled one, with the current magnitude allowed through controlled by firing angle α. Image from [29], page 10.

be used in isolation. SVCs are principally used for voltage control and power oscillation damping, though they can be used in many other ways as well [31]. SVC integration into a power system needs to take certain factors into account. If not controlled correctly or not fitted with appropriately tuned filters, an SVC looking solely at voltage compensation can cause or exacerbate current harmonics in a system, which can cause heating problems and reduce power quality [20].

3.2.2 Alternative VAR Compensation Devices

There are many devices focused on providing reactive power compensation, each with varying pros and cons. Syncrhonous generators have been in operation for many decades and are still widely used today [6, 30], while the unified power flow controller (UPFC) is still quite new and largely unimplemented, despite the promising technical flexibility it has [19]. One of the most relevant modern designs of VAR compensation is the static synchronous compensator, or STATCOM.

Much like an SVC, a STATCOM is a shunt connected power electronic device that provides reactive power compensation, among other things [19]; however, while the implementation and performance goals may be similar, a STATCOM operates on entirely different principles than an SVC. In general, it is a solid-state switching converter that has independently controllable output terminals which can generate or absorb reactive power when supplied with energy from a DC voltage source in the form of a dedicated capacitor. It is dimensionally smaller than an SVC, does not rely on passive external circuitry such as reactor and capacitor banks, and is functionally superior to SVCs in most respects [22].

STATCOMs provide their reactive power generation and absorption entirely through electronic processing of voltage and current waveforms in a voltage-source converter (VSC) [19]. Reactive power exchanged with the system is regulated by varying the amplitude of the 3-phase output voltage of the converter. If the output voltage has higher amplitude than the bus voltage, then current flows from converter to the power system, generating capacitive-reactive power. If it is lower, current flows from the system to the converter, absorbing inductive-reactive power. If the voltages are the same, no current flows and the STATCOM is effectively in a standby, or floating, state. Additionally, adjusting voltage phase instead of amplitude can provide real power compensation from its own DC capacitor to the system.

Under pure performance considerations, STATCOMs would appear to make a more ideal actuator for the proposed frequency regulation scheme. It is very possible that such a scheme may one day be developed, but in papers as recent as 2015-2016, STATCOMs are considered to be more expensive than and not as widespread as SVCs [20, 21]. While it is difficult to know exact statistics on current prices and near-future projections of the number of units in use in modern power grids, it is very possible that STATCOMs will become a more relevant actuator for VAR compensation-based frequency damping schemes in the near future. With that possibility acknowledgmed, SVCs are still regarded

as the more common type of device at the present time.

3.2.3 Phasor Measurement Unit

PMUs report their measurements at a much faster rate than traditional SCADA sensors, usually at 30-60 samples per cycle, as compared to the 2-4 spc of traditional SCADA [28]. The ability to GPS time-stamp their measurements allow for very accurate measurements across large areas to be taken, allowing operators to more easily detect voltage instabilities, validate load models, improve on state estimation, analyze system events, and detect oscillations within the system [32]. The ability to detect electrical oscillations across a wide area is of increasing importance as transmission systems must compensate for higher proportions of RES in power grids.

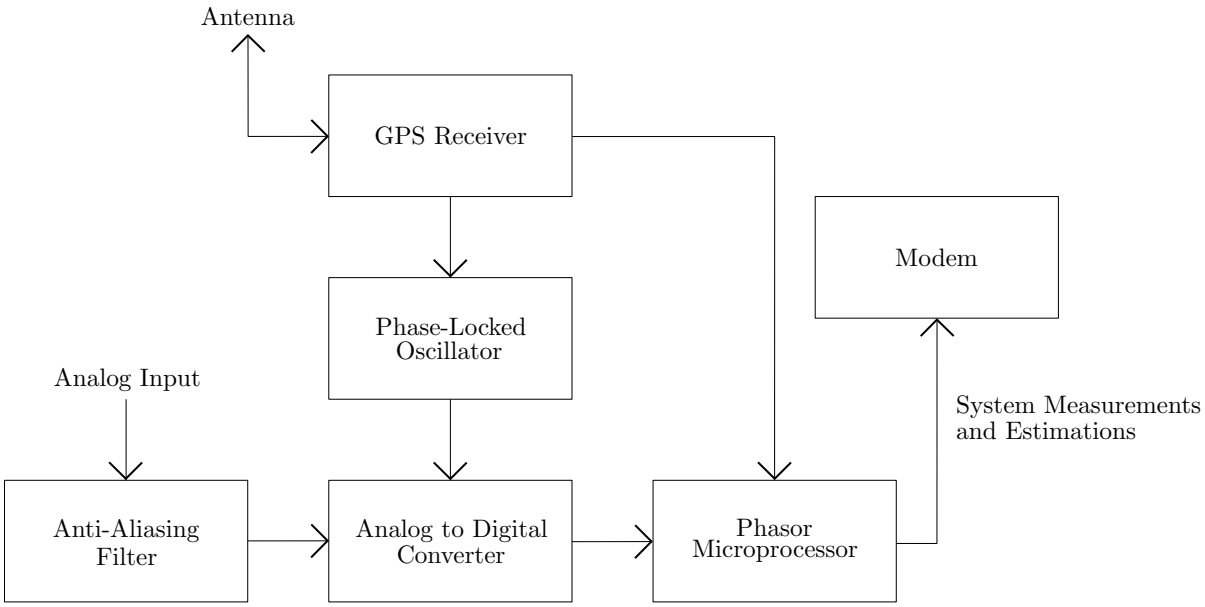

Figure 3.2: Block diagram of a PMU with generic functionality.

In a large electrical grid system, power can be transferred across large distances from generator to load. All generators on a grid need to operate at synchronized turbine speeds, which is 60 Hz in North America. If one or more generators in a large system disconnects from the grid, automated controllers monitoring grid conditions will adjust the output from other generators to compensate. As multiple generators try to match each other

through repeated increasing and decreasing of turbine speeds, frequency oscillations in the power signals across a wide area are created. If the oscillations are small, then it is likely that the swing will decay and operation will return to steady-state with no incident, but if it is large, or if there are other factors besides turbine speed that are contributing to the oscillations, protective relays can be tripped, equipment damaged, and power systems can experience cascading blackouts in extreme cases [32].

Such oscillations can be damped out by frequency control devices, but the feedback control designs that these devices use rely on sensor accuracy to function properly, as sensor noise cannot be easily designed around in a control law [33]. With PMUs offering around ten times the sampling rate of traditional SCADA sensors [28] as well as the ability to coordinate measurements across a wide area, protective control schemes can become proportionally more detailed and effective in regards to sensor limitations. The PMU also measures both frequency and voltage simultaneously in order to produce a phasor, providing engineers with a single device that can facilitate the sensor role for multiple control laws.

3.3 Model Assumptions and Estimation

The basis behind the proposed SVC-based frequency compensator is to use fundamental elements of control theory, specifically Bode loop shaping techniques [33], to create a filter that can emphasize control actions on oscillatory responses specific to the system the SVC is attached to. In order to do that, system's frequency response function must be estimated. The techniques best suited for any individual system identification effort depend on the system in question, but a broadly applicable technique for identifying oscillations within a poorly mathematically defined system is that of non-parametric broadband PSD estimation [34], where the system is excited across the whole power spectrum and the resultant response is displayed and analyzed. The mathematical basis behind this technique of system identification is provided, but all that is required on a

practical level is a knowledge of the sensor bandwidth (i.e. Nyquist or cutoff frequency) and the ability to perform Fourier signal analysis.

First, it is necessary to determine whether system identification will follow a parametric or non-parametric approach [34]. Non-parametric does not mean a model has no parameters. They are usually characterized by having a large number of unknowns. When the response coefficients of a system are directly estimated by observing the response of the system to various inputs, this is non-parametric identification. Parametric models possess fewer parameters and require previous, but not necessarily perfect, knowledge of the system. The parameters are what are estimated, not just the response of the system, which requires there to be fewer unknowns. The development of the proposed SVC frequency compensator follows a non-parametric estimation approach, as the modified IEEE 12 bus model, presented in more detail later, has many unknowns and is approached with minimal existing knowledge of the system dynamics.

For both types of models, estimation and analysis can then follow either a time-domain or frequency-domain description. For the description presented here, the frequency domain will be given preeminent consideration, as the frequency domain is what is used to measure the primary performance criterion for voltage frequency control, namely how effectively the SVC frequency compensator damps the system frequency modes while maintaining voltage regulation. The following derivations are summarized from [34].

The composite model of a system attempts to unify the deterministic and random, or stochastic, components of a system. It describes the combination of deterministic and probabilistic effects for input $u[k]$ and output measurement $y[k]$.

$$y[k] = Gu[k] + He[k] \tag{3.1}$$

This model is non-parametric when G and H are represented in a non-parametric form, i.e. they are not represented by specific parameters. They are instead usually described by their responses to inputs. The notation in Equation (3.1) is to be understood

as "G operating on u" and likewise for He, not as multiplication. G is the plant model and H is the noise model, where e is white noise. If G and H are non-parametric, then they are inferred based on the relationship between input $u[k]$ and output $y[k]$. The underlying assumptions for estimating a composite model are:

- The noise e is additive;
- The deterministic portion of the system, G, or at least the relevant operating point, is linear and time-invariant (LTI); and
- The stochastic signal is stationary and can be expressed as the output of an LTI system driven by white noise.

The definitions for a "stationary" signal are different for a stochastic signal than for a signal with both deterministic and stochastic components. The time average of a stationary signal must stay within a finite range over time and converge to some value, i.e. its average value is bounded with respect to time, or it has a bounded time average. In the general case, the deterministic portion of the composite model produces a signal that changes with time, meaning that a composite model made up of both deterministic and stochastic components is not stationary, invalidating one of the assumptions necessary for estimating it. However, if the signal of the deterministic component is "well behaved" over long periods of time, the ensemble average will have bounded time averages. The requirements for being "well behaved" essentially equate to meeting the definition for being "quasi-stationary." Thus, in order to employ non-parametric broadband PSD estimation, the definition for "quasi-stationary" signals will be given.

A generalized expectation operator for combined deterministic and stochastic signals is defined as

$$\bar{E}(f(s[k])) = \lim_{N\to\infty} \frac{1}{N} \sum_{k=1}^{N} E(f(s[k])) \tag{3.2}$$

This generalized operator facilitates both purely stochastic stationary signals and deterministic signals. Where $f(s[k])$ is the composite signal, if $f(s[k])$ is stochastic and

stationary, $\bar{E}$ simply becomes the regular expectation operator $E(f(s[k])$, and if $f(s[k])$ is deterministic, $\bar{E}$ becomes the time average of all signals.

This leads to the auto-covariance function (ACVF) of the signal

$$R_{ss}[k,m] \equiv E(s[k]s[m]) \tag{3.3}$$

And the large sample ACVF

$$\bar{R}_{ss}[k,m] \equiv \bar{E}(s[k]s[m]) = \lim_{N\to\infty} \frac{1}{N} \sum_{k=1}^{N} R_{ss}(k,m) \tag{3.4}$$

Where $s[k]$ is once again a composite deterministic/stochastic signal and $s[m]$ is a second sample signal of identical type. If this covariance is bounded for all values of k and m, and the limit is only a function of the lag between signals, or $l = k - m$, meaning

$$\bar{R}_{ss}[k,m] = \bar{R}_{ss}[k-m] = \bar{R}_{ss}[l] \tag{3.5}$$

then $s[k]$ is quasi-stationary. The primary motivation behind defining a quasi-stationary signal is to provide a formal definition for the criteria necessary for practically performing system identification. Using this definition, stationary stochastic signals are also quasi-stationary.

There are some key practical signals that fall under the definition of quasi-stationary. First, there are periodic deterministic signals. This includes sinusoids and the full sequence of a pseudo-random binary sequence, among others. Finite aperiodic deterministic signals are not quasi-stationary. Second, there are random stationary signals, the most relevant of which is the finite-length realization of white-noise, which importantly has zero mean, by definition.

As with stationary signals, a quasi-stationary signal can be characterized by a PSD,

$$\gamma_{ss}(\omega) = \frac{1}{2\pi} \sum_{l=-\infty}^{l=-\infty} \bar{R}_{ss}[l] e^{-j\omega l} \tag{3.6}$$

The periodogram of $y[k]$ is an unbiased estimator of the PSD for a stationary signal, and the same holds true for the PSD of a quasi-stationary signal, with smoothing necessary for consistency in both cases.

The same is true for pairs of quasi-stationary signals, namely

$$\gamma_{yu}(\omega) = \frac{1}{2\pi} \sum_{l=-\infty}^{l=\infty} \bar{R}_{yu}[l] e^{-j\omega l} \tag{3.7}$$

The theorem showing that the output of an LTI system excited by a quasi-stationary signal is also quasi-stationary is as follows [34]:

Theorem 1

Let $G(q^{-1})$ be a stable transfer function and $u[k]$ be a discrete-time quasi-stationary signal with spectral density $\gamma_{uu}(\omega)$. Then the signal

$$s[k] = G(q^{-1}u[k]) \tag{3.8}$$

is also quasi-stationary with

$$\gamma_{ss}(\omega) = |G(e^{-j\omega})|^2 \gamma_{uu}(\omega) \tag{3.9a}$$

$$\gamma_{su}(\omega) = G(e^{-j\omega}) \gamma_{uu}(\omega) \tag{3.9b}$$

This leads back to the initial definition of a general LTI system (3.1) being classifiable as quasi-stationary provided the following are true:

- The filters G and H are stable.

- The input $u[k]$ is quasi-stationary (deterministic).
- $e[k]$ is a zero-mean white-noise process with variance σ_e^2.

The frequency domain general definition of a quasi-stationary LTI model can be described either via signal description or spectral description. The spectral description is used here as it leads to identifying the system through estimating the disturbance spectrum. The goal is to use input-output data to develop a frequency response function for the non-parametric model. The following model applies when the LTI system disturbance is measured *open-loop*:

$$\gamma_{yy}(\omega) = |G(e^{j\omega})|^2 \gamma_{uu}(\omega) + \gamma_{vv}(\omega) \tag{3.10}$$

While a more thorough system identification effort would likely use the non-parametric model of the system as the foundation for constructing a parametric model, such efforts are unnecessary in this context. The ultimate goal of the proposed SVC frequency regulator is to improve the frequency oscillation damping of the power system it is implemented in with minimal configuration requirements, utilizing hardware already existing on many modern power systems. Once a good estimate of the frequency response of the system is developed, that frequency response will become the primary criterion against which the efficacy of the controller is judged.

3.3.1 Test Model System Identification

In practical applications, control systems are installed on already existing power systems that have many interdependent parts. The design process to develop this compensator sought to mirror the reality of installing new control components as closely as possible. Thus, the decision to use a slightly modified generic IEEE 12-bus test system was made before controller design started, and the SVC frequency compensator was designed around its unique dynamics and standard operating points caused by the wind farm that was

added to the model. The method of system identification used is general enough to apply to virtually any power system and provide direct comparisons for various states of the power system (e.g. with or without the proposed compensator, higher or lower disturbance signals).

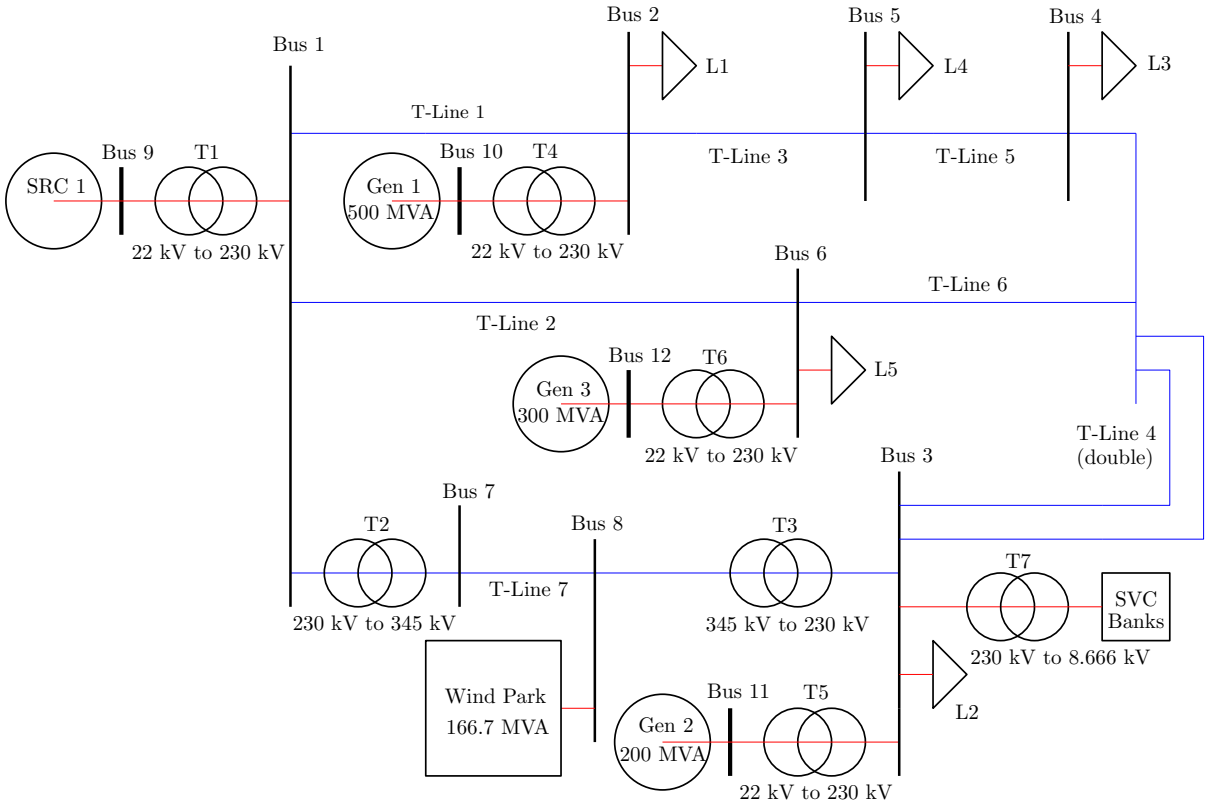

Figure 3.3: Modified IEEE 12 bus system with wind park and SVC banks

The generic IEEE 12-bus model has 3 synchronous generators and one ideal source representing a stiff connection to a larger grid. None of the synchronous generators are operating with power system stabilizers, which allows the primary damping capabilities of the proposed frequency regulator be seen, but also does not take potential interactions between the proposed regulator and standard PSS operation into account. A 166.7 MVA wind farm with 100 turbines was added to the model in order to test the effects of the regulator on a system with significant RES presence. The model was built and tested on the Real-Time Digital Simulator (RTDS) platform. All tests performed and data gathered were done in real-time, simulating hardware dynamics and limitations.

In order to develop a compensator that can continuously modify the SVC to control for frequency deviations in addition to voltage deviations, an estimate of the frequency response function (FRF) of the system must be established. To that end, non-parametric broadband PSD estimation is employed and Welch periodograms of the PSD FRF are made.

Referring back to equation (3.9b), the estimation of the FRF, $G(e^{j\omega})$, is what is solved for [34]:

$$\gamma_{yu}(\omega) = G(e^{j\omega})\gamma_{uu}(\omega) \tag{3.11}$$

$$\Longrightarrow G(e^{j\omega}) = \frac{\gamma_{yu}(\omega)}{\gamma_{uu}(\omega)} \tag{3.12}$$

where $G(e^{j\omega}) \longrightarrow \hat{G}(e^{j\omega})$ once an estimator is reached. It bears repeating that only when using smoothed estimators is a consistent FRF estimation reached.

The validity of the FRF estimates are also limited by the sampling rate of the sensor used to gather the data, in this case the PMU. Signal processing of any kind is bandwidth limited to half of the sampling rate, a principle referred to as the Nyquist frequency, or folding frequency. Where the PMU in the current test system is set to have a reporting rate of 30 samples per second, the periodograms are only valid out to 15 Hz. Any data on the frequency response plots past 15 Hz are subject to aliasing, thus missing the actual behavior of the signal beyond that frequency. For the purposes of detecting low-frequency oscillatory responses in power systems, this Nyquist frequency is more than sufficient, as the low frequency oscillations present in power grids usually range between 0.4 to 2.0 Hz, depending on the scale of the system in question [8]. Local modes (i.e. between nearby plants) tend to range from 0.7 to 2.0 Hz, whereas inter-area oscillations (i.e. between large groups of generators, such as the case with WECC or other regional authorities) tend to range between 0.4 and 0.7 Hz.

The next step in system identification is to generate a disturbance signal that excites all frequencies within the control bandwidth and record the frequency response of the

system when the disturbance is applied. The disturbance signal must be of sufficient magnitude to overcome any inherent stability due to inertia and other systems considered as part of the plant, otherwise the system will not exhibit any response behaviors to analyze. The frequency response signal is then put through a Fourier Transform to break it into the relative magnitudes of its constituent frequencies. In the present 12-bus model, the disturbance is created by modulating the dynamic load on Bus 3 with additive white Gaussian noise (AWGN) until the frequency signal measured by the PMU oscillates at ± 0.1 Hz from 60 Hz. Because the load disturbance is created by AWGN, the linearity of the system is maintained. AWGN also has a constant PSD, and excites the system equally across all frequencies.

Disturbing the load with AWGN has several beneficial properties:

- The linearity of system operating point is maintained, as the noise is *additive*;
- Noise that is *white* excites the system across all frequencies equally which allows the system to respond at all frequencies without affecting the system's PSD; and
- *Gaussian* noise has a probability density function equal to a Gaussian distribution, which allows for consistent noise signals across large collection periods.

Taken together, disturbing the system with AWGN excites any modes inherent to the system and shows at what frequencies they oscillate with rest of the system. This identifies the frequencies that experience major oscillations.

As discussed earlier, when using non-parametric broadband PSD estimation, multiple estimations must be averaged together in order to create a consistent estimator. In this case, the periodograms are the Discrete Time Fourier Transform of the steady-state system frequency response to the AWGN disturbance signal. By averaging many samples of the DTFT of these frequency responses, a smoothed, consistent estimation of the actual FRF of the system is reached. This averaged, smoothed periodogram is known as a Welch Periodogram. The more periodograms that are used to create the Welch Periodogram,

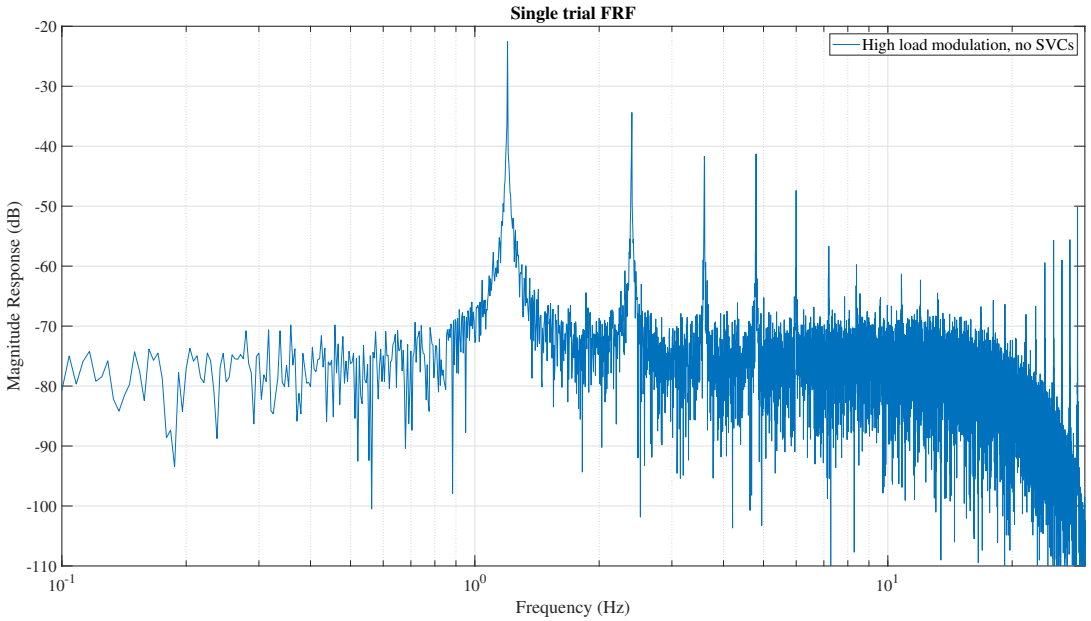

Figure 3.4: Estimated Frequency Response Function after 4 minutes of system excitation

the less variance there is in the FRF estimator.

In this case, each of the FRF estimators for different conditions were created using an average of 6 frequency response periodograms. This is a sufficient number to prove a basic level of consistency within the responses while still allowing for many different system conditions to be tested. The difference between the base FRF with only one periodogram and the Welch periodogram of 6 trials of 4 minutes of continuous data each is readily apparent.

The smoothed FRF estimation of Figure 3.5 shows a frequency oscillation at $\omega_m = 1.2$ Hz along with multiple harmonics of that oscillation. It is possible, perhaps even likely, that this oscillation coincides with one of the natural modes of the wind parks, but further identification efforts would be needed to confirm that. Any analysis of the periodograms must stop at the Nyquist frequency of $\omega_{nyq} = 15$ Hz, though the plots continue to 30 Hz for increased readability. These graphs show the system with no power system stabilizers and no SVC banks. Once the mode has been identified, a compensator may be designed to damp these harmonics. It should be noted that in this and other

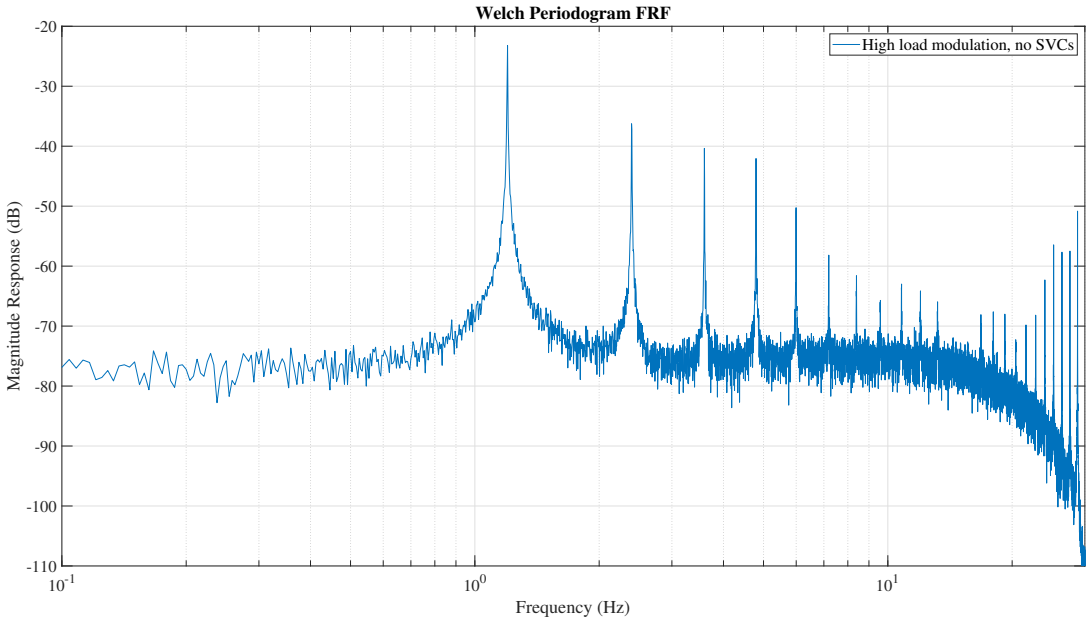

Figure 3.5: Smoothed Frequency Response Function estimation, using 24 minutes of data

periodograms throughout this thesis that the dB scale used is not normalized, as the metric of performance, namely the how effectively the frequency oscillations are damped, is relative. The relative scale is the same for all graphs, and the performance of the frequency regulator is well illustrated by the relative scale.

3.4 Simulated SVC Component

The main design goal of the controller developed is to provide adequate levels of frequency oscillation damping while maintaining an SVC bank's ability to regulate voltage magnitude. To that end, the primary control loop of the SVCs are left unmodified, where the only exception is the location the filtered frequency measurement is injected into the SVCs' existing control signal. An description of the SVCs' control loop is warranted to understand the motivations behind the frequency regulators' implementation.

From a controls perspective, the SVCs work by measuring bus voltage magnitude and calculating a susceptance value which is then scaled to the SVCs' nameplate rating,

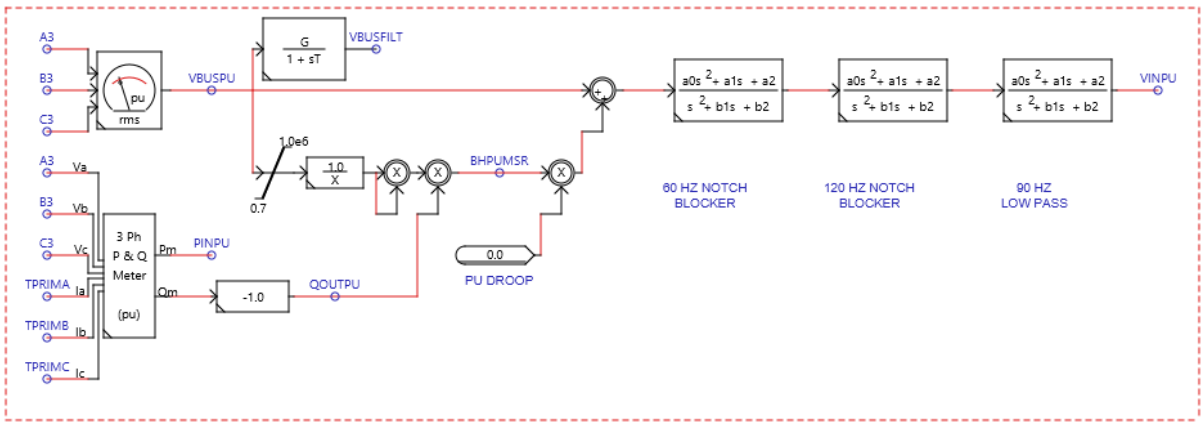

Figure 3.6: Voltage measurement block of native SVC controls

linearized, and calculated into a firing angle. Figure 3.6 illustrates the process of measuring the voltage from Bus 3 on the 12-bus system and filtering the measurement. This bus is separated from the where the wind park attaches to the transmission system by a step down transformer, and is also next to a synchronous generator and dynamic load, making it a highly dynamic bus on which to test the frequency controller.

The initial measuring and filtering process shown in Figure 3.6 also provides a means of compensating the voltage measurement with droop, which is not utilized in the present system so that the full range of regulator bandwidth may be used for testing. Thus, the effective filtering process is to simply pass the RMS bus voltage through two notch filters and a low pass filter. This voltage input then goes through the actual control loop of the SVC banks, as shown in Figure 3.7. There are means by which to run the SVCs using arbitrary values, seen by the "DEBLOCK" and "BSETMOD" switches, which are primarily used for simulation startup.

The filtered voltage signal is passed through a proportional-integral (PI) controller, the results of which are passed through a saturation function and referred to as a susceptance value, denoting the voltage deviation from the reference. This serves as the first of two potential saturation points in the SVC, an issue which is relevant in the present testing environment. This susceptance signal then goes through several calculations to determine what value is linearized and converted into firing angle α. Some amount of

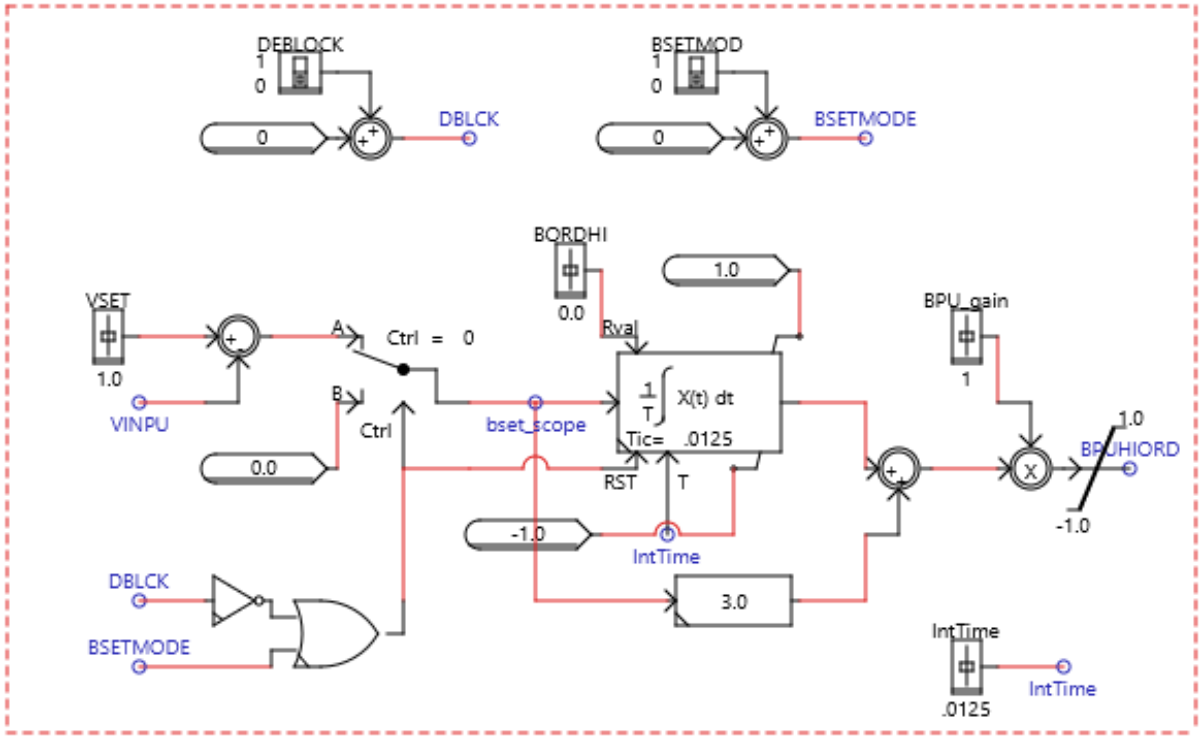

Figure 3.7: PI controller uses measured voltage change to infer change of susceptance

transformer leakage is assumed, and the firing angle changes based on whether the TSC component of the SVC bank fired or not on the last cycle. It is here that the frequency compensator's control signal is injected, after all adjustments have been made the to susceptance value for the voltage control signal. Injecting the control signal at this point ensures that original control law of the SVC as it relates to voltage regulation is unaffected.

From there, the value is converted into a power signal appropriate to the nameplate rating of the TCR portion of the SVC bank, linearized, and calculated into a firing angle, as seen in Figure 3.8. It is once again key to notice the saturation block. This along with the linearization function ensures that the firing angle of the SVCs stay between 90° and 180°, so when the signal saturates, it means that the SVC is injecting or absorbing as much reactive power as it is capable of.

The firing angle α is then used by the firing pulse generator of the TCR component of the SVC. The TSC component activates based on the voltage of the measured bus,

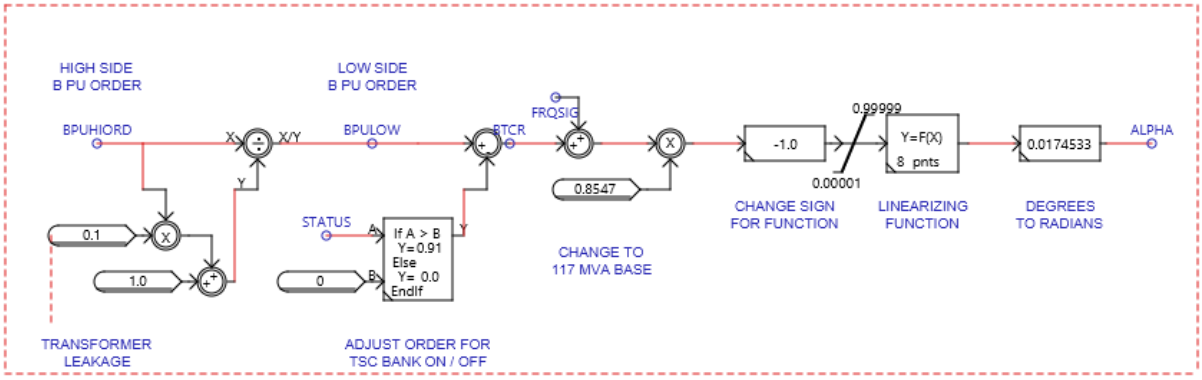

Figure 3.8: Control signal (susceptance + frequency) is linearized into firing angle α

which in this configuration carries through to the TSC firing block as a segment of the susceptance manipulation process, denoted as "BPULOW" in Figures 3.8 and 3.10. The TCR also measures the phase from the bus via a phase-lock loop. The TCR firing pulse generator must be configured to ensure it is receiving and sending signals with the correct amount of phase, taking transformer lead or lag into account when setting control based lead and lag settings. In the case of this system, the firing pulse generator is required to have a 30° lead on Bus 3.

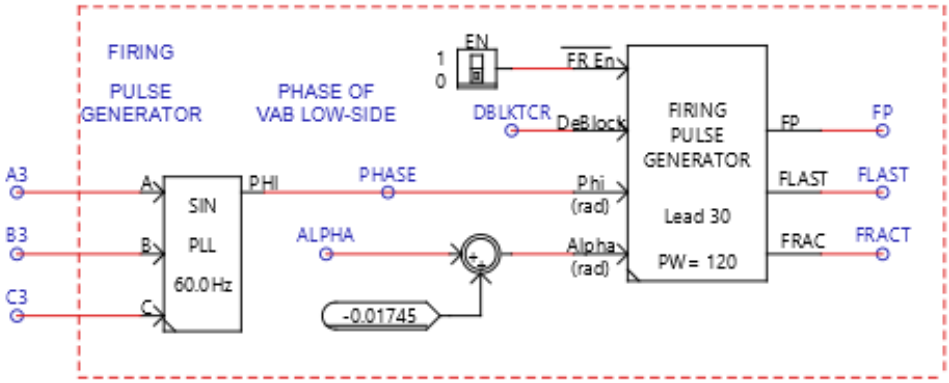

Figure 3.9: TCR firing block

When the SVC is only regulating bus voltage, it marginally improves the frequency response of the system. As can be seen in Figure 3.11, the magnitudes of the primary frequency oscillation and its subsequent harmonics are slightly lower, but also shifted up in frequency. The amount of load modulation necessary to cause the wind parks to

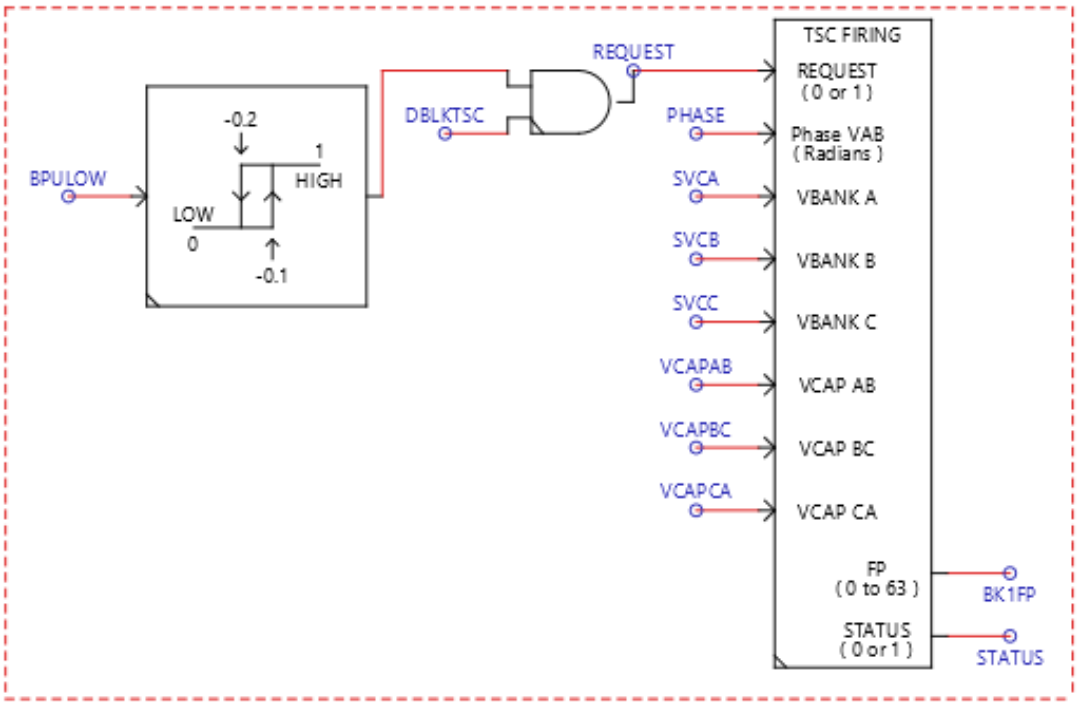

Figure 3.10: TSC firing block

exhibit oscillations does increase with the SVC only regulating voltage versus having no SVCs attached at all, but ultimately, if a fault or load imbalance were to cause an oscillation of sufficient magnitude in the system, voltage controls would be insufficient for maintaining a frequency stability within the system.

3.5 Frequency Compensator

With system oscillatory frequencies identified, the target frequencies for the proposed regulator to damp are now known. The frequency regulator will use the SVC as the actuator in the control loop, and an appropriate point to interface with the actuator must be determined. As has been mentioned previously and shown in Figure 3.8, the site chosen to inject the frequency control signal is directly before the voltage control signal, in the form of a susceptance value, begins its calculation into the firing angle α. This has two major effects:

- The control signal calculations taking place for the voltage signal is unaffected, and

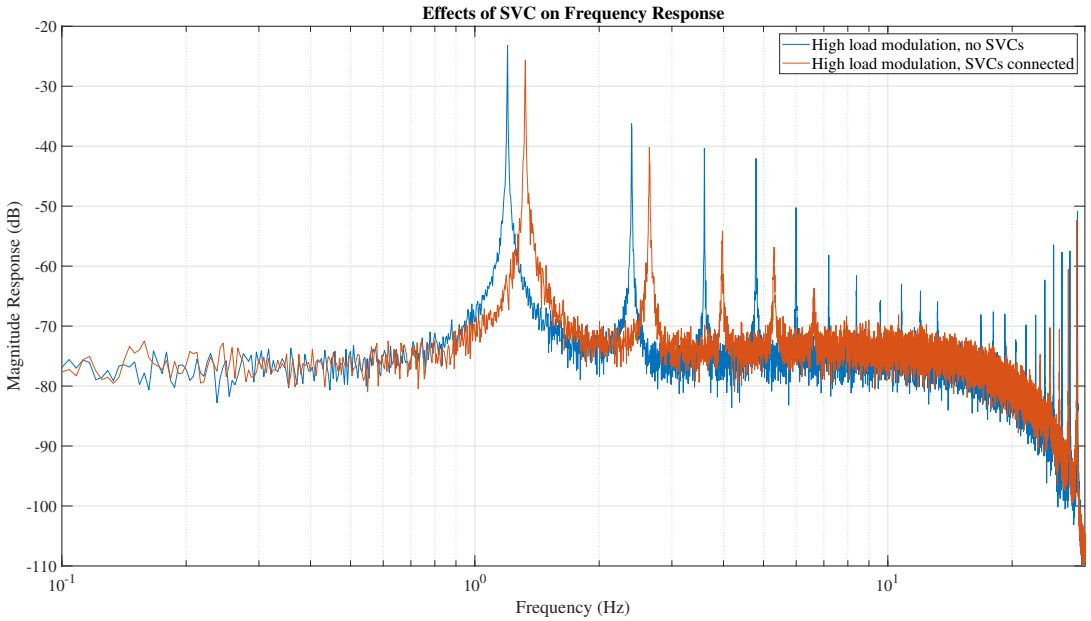

Figure 3.11: The SVC controlling only for voltage minimally damps small signal frequency oscillations

- The SVC controls simultaneously for voltage and frequency, modulating equally as much due to voltage measurements irregardless of the frequency compensator's presence.

This state of simultaneously controlling for voltage and frequency is beneficial because the frequency compensator will only affect SVC operation by any noticeable amount when frequency begins to fluctuate significantly, and requires no additional computational elements to determine when to activate. It also comes with the drawback that if the SVC rating is too low or the system it is supporting requires significant voltage support, then the amount of actuator capacity available may significantly limit control bandwidth. Such is the case in the modified IEEE 12-bus test system used for this design process. When the system is disturbed, and before any frequency regulation signal is applied, the amount of voltage regulation the SVC provides nearly saturates at both the initial PI voltage controller that produced a per unit susceptance value as well as the linearization function that determined α. In modifying the test system to include a wind park of

significant size, the voltage balance of the overall system is adversely affected, especially when the system is disturbed via load modulation, resulting in the SVC regulating voltage to its maximum actuation bandwidth.

To compensate for this and allow for the frequency regulator to have sufficient actuator bandwidth to function in the present test system, the susceptance calculation that results from the PI control blocks is throttled, visible as the component "BPU_gain" in Figure 3.7. This throttle is set to reduce the voltage regulation signal to 70% of its calculated value in order to free up actuator bandwidth that the frequency regulator can utilize. It bears emphasizing that this is not a typical situation for SVCs operating in power grid transmission systems, but one of the goals in designing the present frequency regulator is to work with the system as is. In more practical environments, SVCs would have ample actuation "headroom" with which to work. None of this alters how the frequency regulator is designed or implemented, and actually shows that it is an effective design even in a situation with limited actuation capacity.

Acknowledging that SVC reactive power capacity must be freed up for this particular test system, the design of the frequency compensator utilizes basic principles of closed loop feedback control, specifically principles of Bode loop shaping [33, 35]. Loop shaping uses the frequency domain representation of a transfer function, often referred to as the Bode plot of the transfer function, and inserts poles and zeros to increase the magnitude of the response and adjust the phase at specific frequencies. By moving the high and low magnitude response frequencies of a closed-loop transfer function through the use of strategically placed poles and zeros, the frequency response of the loop is "shaped" to have the desired response characteristics, and sufficient phase margins are achieved. The desired characteristics for the Bode plot of the proposed SVC-based frequency regulator's frequency feedback controller are:

- Have relatively high magnitude feedback at the frequency of the mode identified via non-parametric broadband PSD estimation,

- Have low magnitude feedback everywhere else and roll off at high frequencies, and
- Maintain an acceptable phase stability margin.

This transfer function would act as a filter on the frequency measurements taken by the PMU, which are compared to a reference (60 Hz in North America) and then produce a control signal that would be added to the voltage control signal. The resulting system is a two-input, single-output controller for the SVC's reactive power injection and absorption.

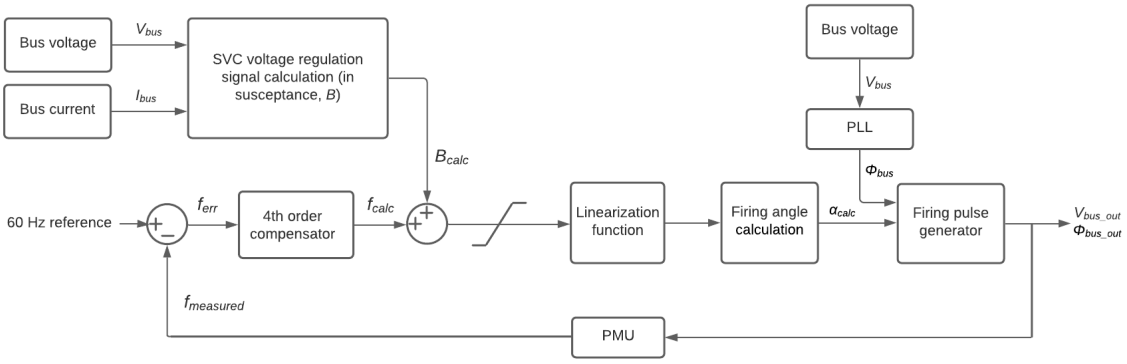

Figure 3.12: Block diagram of the SVC's frequency control loop, showing where existing control considerations intersect with it.

However, because the frequency compensator does not take the voltage tracking directly into account, only insofar as the SVC is changing the system state via voltage regulation, the susceptance signal also used for controlling the SVC functions as an additive control input in the frequency control loop. This reduces the SVC frequency control loop to look as it does in Figure 3.13.

The frequency compensator transfer function for the controller is

$$C(s) = \frac{10s^3 + 155s^2 + 310s + 1400}{s^4 + 29.8s^3 + 228.4s^2 + 792s + 2880} \tag{3.13}$$

or, in terms of poles and zeros,

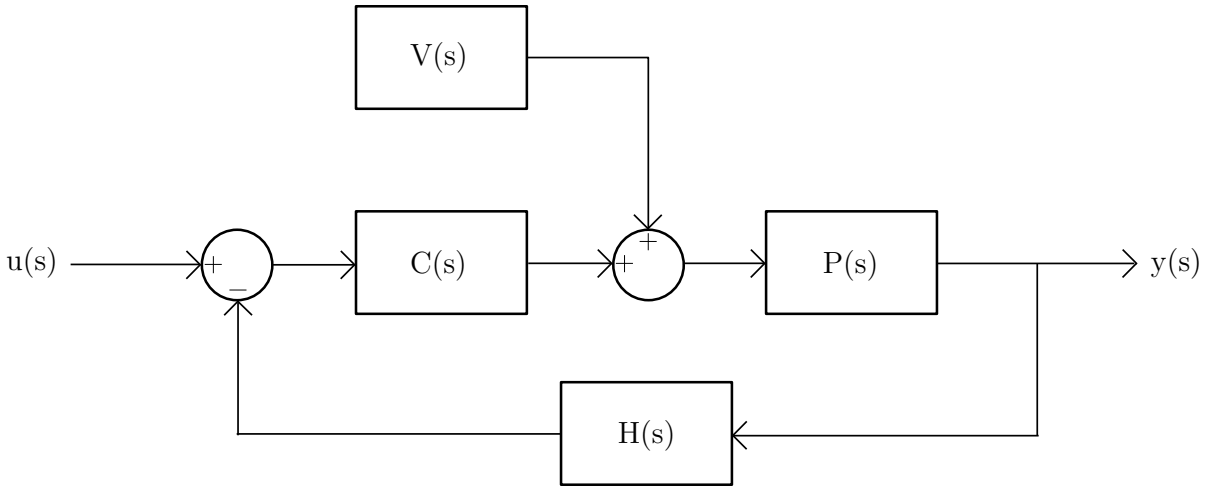

Figure 3.13: Block diagram of the SVC's frequency control loop reduced down to basic control components.

$$C(s) = \frac{10(s+14)(s^2+1.5s+10)}{(s+20)(s+8)(s^2+1.8s+18)}. \tag{3.14}$$

The transfer function representations of $P(s)$ is not known, and as such a full representation of the loop transfer function $T(s) = C(s)P(s)H(s)$ is not known. The Bode plot representation of $C(s)$ is shown in Figure 3.14.

A complex pair of zeros provides a short reduction in magnitude response before increasing the response by 40 dB/decade, while a complex pair of poles does the opposite, providing a short increase in magnitude response before decreasing the response by 40 dB/decade. Putting the complex zero pair slightly before the complex pole pair in relation to both the real and $j\omega$ axes means that there is a very gentle increase in the magnitude response that peaks just before the frequency of the mode compensated for. The pole at $s = -8$, the zero at $s = -14$, and the pole at $s = -20$ then provide a gradual decline of magnitude and phase angle that terminates in high order response roll off and $-90°$ of phase, well within stability limits.

As noted earlier, Figure 3.14 only represents the transfer function of the frequency compensator $C(s)$, not the full loop transfer function of the frequency control system, $T(s)$. The transfer function underwent several numerical variations that all used the

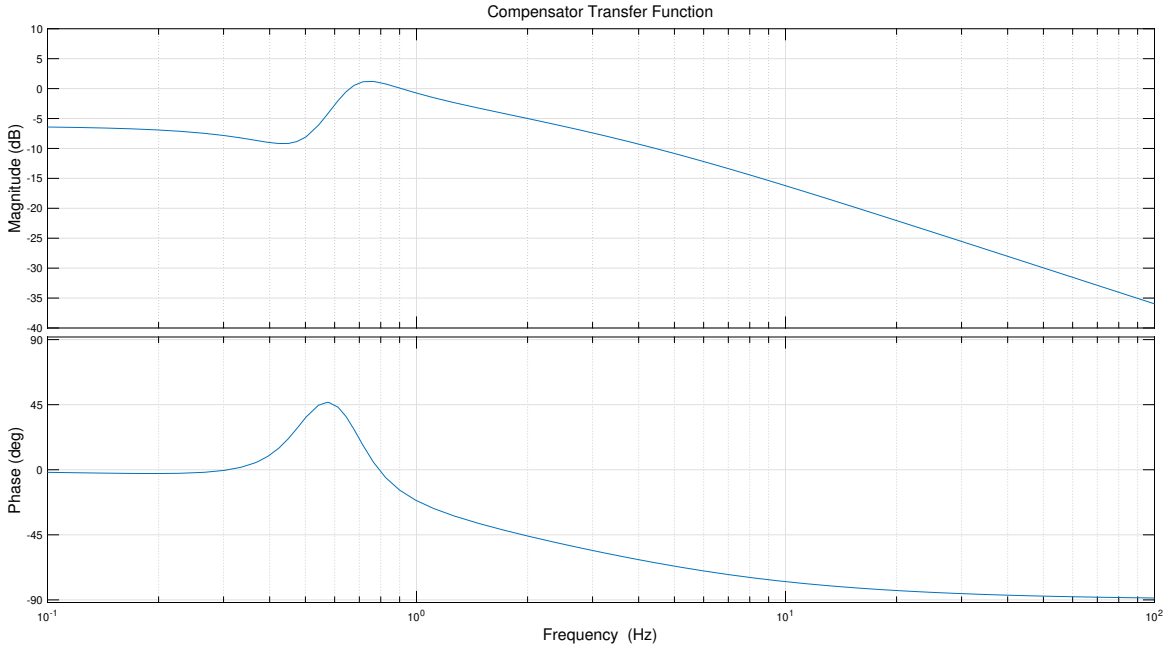

Figure 3.14: Bode plot of transfer function $C(s)$.

same principles of gentle gain increase at the mode frequency and gradual roll off at high frequencies to arrive at the present function.

Using a transfer function as a filter on the PMU's measurement signal is the most novel part of the frequency compensator's design. It requires negligible amounts of additional computational power and simply emphasizes control action on the previously identified frequencies that exhibit the largest oscillatory response, only practically affecting the operation of the SVC when the frequencies in question are excited. There are no decision making mechanisms to malfunction, and through the use of very basic techniques of system identification and transfer function design, the performance of the frequency response of the system is dramatically increased.

Chapter 4: Results

In order to minimize system complexity, the frequency regulator described in the previous section must be able to function as an always-on compensator that does not affect the normal operations of the SVC. Figure 4.1 shows the FRF of the modified IEEE 12-bus test system as it operates under load disturbances that put it at the boundary of nominal conditions, referred to hereafter as "marginally nominal," and frequency deviations are within ± 0.04 Hz. The system is tested at the boundaries of nominal operation in order to provide some amount of frequency response dynamics for the sake of visibility in the results. If the system is well within nominal operating conditions, there would be no visible frequency response to compare relative performance at various operating conditions against. As was described earlier, the SVC provides significant voltage support even during marginally nominal operation due to the lack of fine tuning of the test system. For all FRF plots, the voltage regulation signal has been reduced to 70% of its calculated value in order to provide control bandwidth to the frequency compensator.

As seen in Figure 3.11, the presence of the SVC bank in the system shifts the primary mode, which is less pronounced with the smaller load modulation, to a slightly higher frequency. It is notable that having the SVC only performing voltage regulation actually decreases the quality of the frequency response of the system, which is discussed at greater length in [36]. When the frequency compensator is active, the damping on the mode improves. At this magnitude of load modulation, the difference in the frequency response at the system mode is not as pronounced as when the wind park controllers begin misoperating due to load imbalance, as shown in Figure 4.2, but there is still an approximately 10 dB reduction in the response. This leads to two conclusions about the proposed frequency regulator when the system is operating at marginally nominal conditions:

- The proposed frequency regulator takes very little control bandwidth when the rest

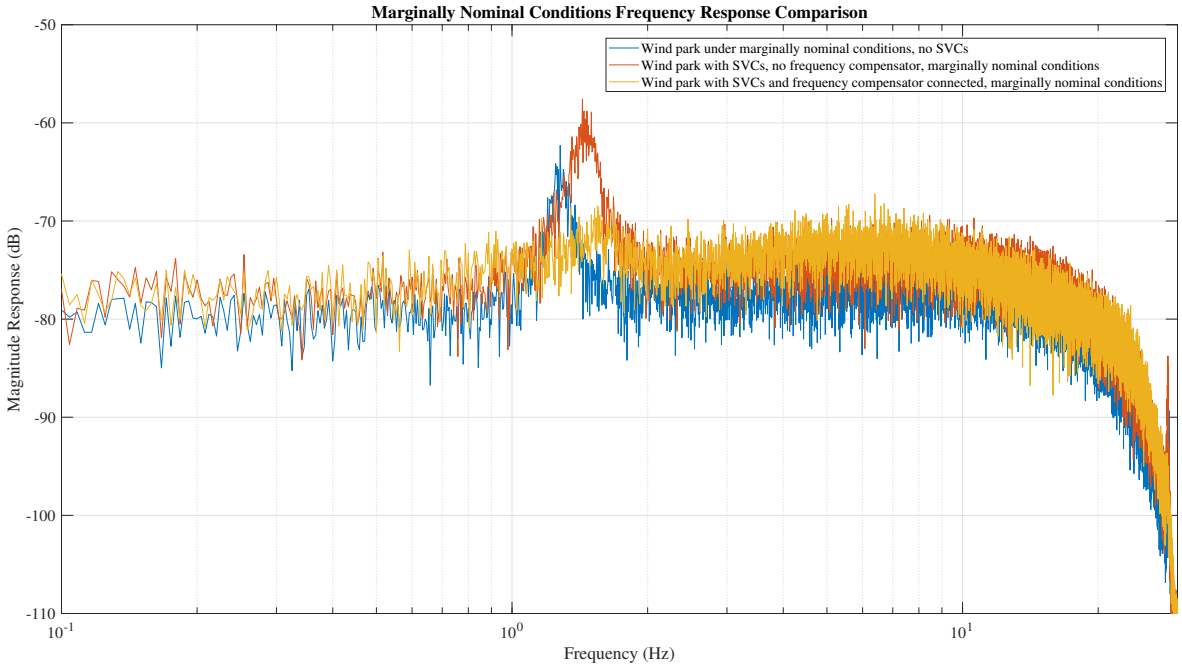

Figure 4.1: Frequency response plot of the system at marginally nominal conditions alone, with an SVC bank without the novel frequency compensator, and with the SVC bank with the novel frequency compensator.

of the system can handle the frequency oscillations occurring due to any number of minor disturbances that are omnipresent in normal power system operations; and

- Even if the system is not under conditions that would otherwise cause frequency collapse, the proposed frequency regulator still noticeably improves the frequency oscillation damping of the system.

This shows that the proposed regulator design works as an always-on protective control element in the SVC.

When the magnitude of load modulation causes the wind park controllers to misoperate and produce significant oscillations, the difference between the system with the frequency regulator versus without become obvious. Figure 3.11 shows the system undergoing large load modulations both with and without the SVC attached, and Figure 4.2 overlays the frequency response of the system under the same conditions with the

frequency regulator on top of the other two responses.

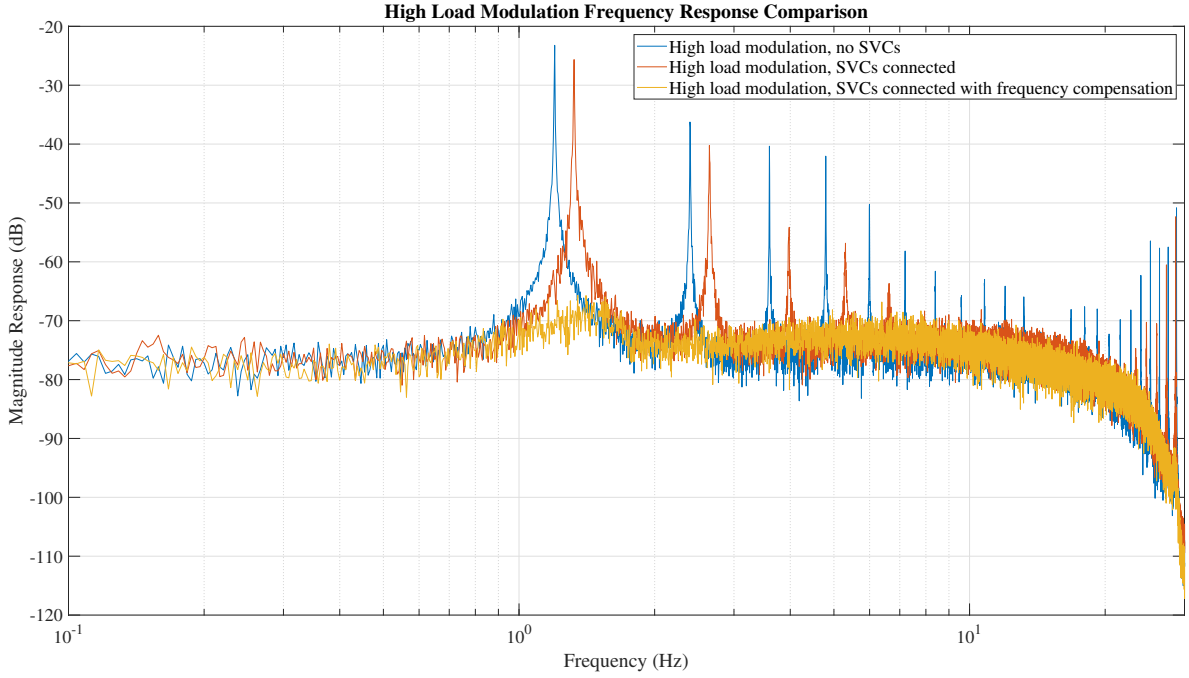

Figure 4.2: Frequency response plot of the system under high load modulation as the base system, with an SVC bank without the novel frequency compensator, and with the SVC bank with the novel frequency compensator.

The SVC-based frequency regulator enables the system to have virtually the same frequency response under high levels of load modulation as it has under marginally nominal conditions. It provides the system with 40 dB damping under these conditions, or a factor of 100 times reduction in amplitude. It also reduces the harmonics of the primary oscillation to the point of being immeasurable. There is a slight increase in the magnitude of the frequency response above approximately 1 Hz compared to the system with no SVC or frequency regulator attached, on the order of 5 dB. This is accomplished without changing any of the control processes within the SVC, only adding to them. The only difference in the experimental setup between the yellow periodograms on the plots of Figure 4.1 and Figure 4.2 is the magnitude of the load modulation applied to the system.

All tests are performed on a system that has no power system stabilizers present on any of the synchronous generators, and the wind park also had no form of frequency

control, only voltage and power factor controls. Thus, the frequency stabilization exhibited by the system in these tests is due solely to the SVC performing reactive power regulation for the purpose of frequency control.

Several other transfer functions were tested to act as the filter for the compensator of the frequency regulator. The other most effective design is shown in Figure 4.3 compared to the current proposed filter design. Both regulators serve to significantly damp the frequency oscillations experienced by the system at high levels of load disturbance, but the earlier design, illustrated in orange in Figure 4.3, is not able to as effectively damp oscillations at the start and end of the range of frequencies that the system exhibits significant oscillatory behavior. The high frequency roll of and relatively slight dB response increase at frequencies beyond 1 Hz remain the same as with the final filter design.

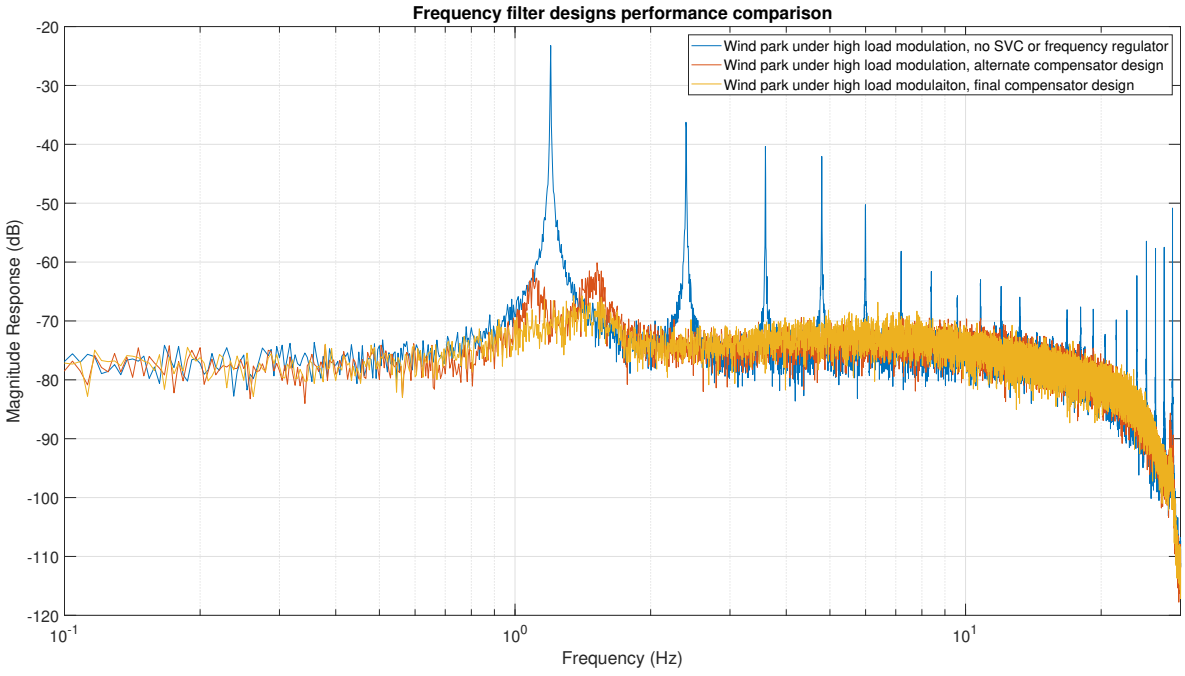

Figure 4.3: Comparison of the two compensators that provided the most damping. An earlier design is shown in orange, the final design is shown in yellow.

An examination of the Bode plots of the two transfer functions provides some insight

into the relative results of the two compensators. Without even knowing the numerical values of the two transfer functions, it can be seen in Figure 4.4 that the earlier design follows a more straightforward design of having low gain early, ramping up to maximize gain at the same frequency as the primary oscillatory response, followed by high order roll off. The phase for the earlier filter is also more dynamic, which potentially contributes to the less consistent damping it achieves, though likely not to a significant degree as the phase margins are always well within 90° for the target frequency range.

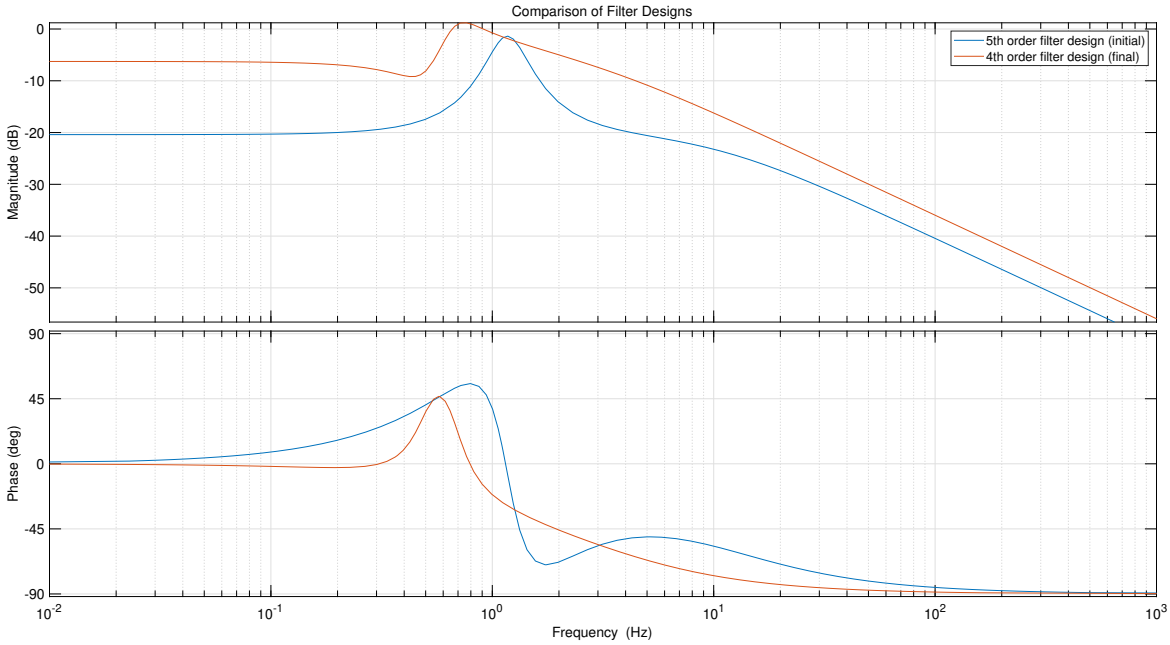

Figure 4.4: Comparison of the Bode plots of the two compensators that provided the most damping. The earlier design is shown in blue, the final design is shown in orange.

The pole-zero representation of the earlier transfer function is

$$C(s) = \frac{6(s^2 + 9.683s + 52.18)(s^2 + 9.917s + 55.96)}{(s + 62.84)(s^2 + 3.328s + 53.63)(s^2 + 3.206s + 54.45)}. \tag{4.1}$$

and it is apparent from comparing it to Equation (3.14) that it is not designed from exact pole and zero placements for relative increases and decreases in magnitude at various frequencies, but rather is numerically generated to have a maximum amount of

gain at 1.2 Hz while maintaining certain other criteria such as phase margins and high order roll off.

The advantages of Bode loop shaping are well illustrated in the comparison. The transfer function that simply focuses on producing high feedback gain at the peak oscillation frequency also has noticeable reductions in damping efficacy immediately before and after the peak frequency. The transfer function that uses Bode loop shaping techniques is able to move some of that feedback response to a lower frequency while maintaining sufficient gain to achieve the same amount of damping at the primary oscillation frequency and superior damping at the frequencies immediately before and after it.

Chapter 5: Conclusion

In this thesis, it has been shown that an SVC can simultaneously run voltage and frequency regulation control loops and perform both functions to a satisfactory degree. This is done on a test system built for other purposes, with a wind park providing a significant amount of power and exhibiting the frequency response issues that are commonly seen in systems with a high amount of RES present [7,36,37]. As long as the basic assumptions of an LTI standard operating point can be met, then the mathematically simple process of non-parametric broadband PSD estimation can be used to identify low frequency system oscillations, and an always-on protective frequency compensator can be designed using basic principles of Bode loop shaping. This regulator acts as an effective primary controller for damping small-signal oscillatory frequency responses while allowing the SVC it affects to provide voltage support at the same time.

This compensator design has been tested for moderate to severe load fluctuations on a moderately sized power system. It should be mentioned that in a realistic scenario, load fluctuations of this magnitude would not be sustained for 4 minutes at a time, as secondary controls would come online to administer additional corrective action, but the efficacy of the regulator was immediately visible in all tests performed. It should theoretically function just as well for any sort of condition or attack that causes frequency fluctuations through reactive power imbalances, but it has not been tested for a wide variety of scenarios yet. Of note, it was briefly tested with a simulated cyber attack on the governor of a synchronous generator, and it had minimal effect. The working hypothesis as to why the frequency regulator was ineffective is that the cyber attack directly changed active power generation and voltage angle, not reactive power generation and voltage magnitude. Further testing and refinement are needed for additional protection cases to be established.

5.1 Future Work

Further work needs to be done on systems of differing sizes, and the effects of distance from the reactive power disturbance to the SVC need to be better examined. The wide-area efficacy of the proposed frequency regulator has not been established, as the test system was simulating disturbances on a local level, only affecting generators within a few busses of each other. Though the relatively simplistic approach to identifying oscillatory frequencies is a valuable part of the research done and an important evidence of the regulator design's applicability, experimenting on more well established models, such as with references [14] or [15], would allow for a more tailored design approach that could better test the performance limits of the proposed SVC-based frequency regulator's implementation scheme. Judging its damping capabilities on inter-area oscillations would necessitate a larger model with well understood inter-area dynamics. PMU sensor dynamics might become more pronounced as multiple devices send measurements from across a large system to data concentrators, increasing sensor delay. Measuring the effect of sensor delay on the frequency regulation feedback loop was not a focus of the present study.

Additionally, testing on a better tuned system or one with more than one SVC bank could lead to more insights on the full damping capabilities of the proposed frequency regulator's implementation. Investigations into any potential dynamics resulting from the interactions between the multiple SVC-based frequency regulators and other SVCs or frequency compensation devices, such as TCSC or STATCOM, should be undertaken. The overall implementation of the compensator into the SVC might be adapted to function with the standard control schemes of other FACTS devices as well, namely that of adding a frequency control signal onto the last step of the respective control processes of those devices. In particular, as STATCOM device design continues to be refined, decreasing their price and thereby increasing their usage in transmission systems, they

would make an ideal actuator for frequency regulation based on reactive power control, as their performance to SVCs is superior in most respects [22].

There are many functions SVCs can perform in power systems [31], and with the increased prevalence of wide-area monitoring systems such as PMUs [14,28], the potential for large scale frequency monitoring and compensation by passive or active elements attached to SVCs is high. Such measures are likely to become only more and more necessary as RES with low generator inertia continue to increase in modern power grid penetration.

References

[1] "1996 System Disturbances," North American Electric Reliability Council, Princeton, NJ 08540-5731, Aug. 2002 [Online]. Available: https://www.nerc.com/pa/rrm/ea/System%20Disturbance%20Reports%20DL/1996SystemDisturbance.pdf

[2] V. Venkatasubramanian and Y. Li, "Analysis of 1996 Western American Electric Blackouts," Bulk Power System Dynamics and Control VI, Aug. 2004 [Online]. Available: https://www.academia.edu/9198860/Analysis_of_1996_Western_American_Electric_Blackouts

[3] "Frequency Instability Problems in North American Interconnections," Energy Sector Planning and Analysis (ESPA), Final DOE/NETL-2011/1473, May 2011 [Online]. Available: https://netl.doe.gov/sites/default/files/Smartgrid/TransmissionFreqProb.pdf

[4] S. Sharma, S. Huang and N. D. R. Sarma, "System Inertial Frequency Response Estimation and Impact of Renewable Resources in ERCOT Interconnection," 2011 *IEEE Power and Energy Society General Meeting,* 2011, pp. 1-6, doi: 10.1109/PES.2011.6038993.

[5] F. Wilches-Bernal, J. H. Chow and J. J. Sanchez-Gasca, "A Fundamental Study of Applying Wind Turbines for Power System Frequency Control," in *IEEE Transactions on Power Systems,* vol. 31, no. 2, pp. 1496-1505, March 2016, doi: 10.1109/TPWRS.2015.2433932.

[6] A. Moeini and I. Kamwa, "Analytical Concepts for Reactive Power Based Primary Frequency Control in Power Systems," *in IEEE Transactions on Power Systems,* vol. 31, no. 6, pp. 4217-4230, Nov. 2016, doi: 10.1109/TPWRS.2015.2511153.

[7] "Black System South Australia 28 September 2016," Australian Energy Market Operator, Mar. 2017 [Online]. Available: https://www.aemo.com.au/-/media/Files/Electricity/NEM/Market_Notices_and_Events/Power_System_Incident_Reports/2017/Integrated-Final-Report-SA-Black-System-28-September-2016.pdf

[8] P. Kundur, *Power System Stability and Control*. New York: McGraw-Hill, 1994.

[9] G. Tsourakis, S. Nanou, and C. Vournas, "A Power System Stabilizer for Variable-Speed Wind Generators," *IFAC Proceedings Volumes,* vol. 44, no. 1, pp. 11713-11719, Jan. 2011, doi: 10.3182/20110828-6-IT-1002.03437. [Online]. Available: https://linkinghub.elsevier.com/retrieve/pii/S1474667016454972. [Accessed: Apr. 14, 2022]

[10] S. Essallah, A. Bouallegue, and A. Khedher, "Integration of automatic voltage regulator and power system stabilizer: small-signal stability in DFIG-based wind farms," *J. Mod. Power Syst. Clean Energy,* vol. 7, no. 5, pp. 1115-1128, Sep. 2019, doi: 10.1007/s40565-019-0539-0. [Online]. Available: http://link.springer.com/10.1007/s40565-019-0539-0. [Accessed: Apr. 14, 2022]

[11] N. Mithulananthan, C. A. Canizares, J. Reeve and G. J. Rogers, "Comparison of PSS, SVC, and STATCOM controllers for damping power system oscillations," in *IEEE Transactions on Power Systems,* vol. 18, no. 2, pp. 786-792, May 2003, doi: 10.1109/TPWRS.2003.811181.

[12] C. Chang and S. Maharjan, "Analysis of damping oscillation using discrete control signals from Phasor Measurement Unit (PMU)," *2015 North American Power Symposium (NAPS),* 2015, pp. 1-5, doi: 10.1109/NAPS.2015.7335198.

[13] J. Quintero and V. Venkatasubramanian, "A Real-Time Wide-Area Control Framework for Mitigating Small-Signal Instability in Large Electric Power Systems," *Proceedings of the 38th Annual Hawaii International Conference on System Sciences,* 2005, pp. 66c-66c, doi: 10.1109/HICSS.2005.43.

[14] D. Roberson and J. F. O'Brien, "Variable Loop Gain Using Excessive Regeneration Detection for a Delayed Wide-Area Control System," in *IEEE Transactions on Smart Grid,* vol. 9, no. 6, pp. 6623-6632, Nov. 2018, doi: 10.1109/TSG.2017.2717449.

[15] B. Pierre et al., "Supervisory system for a wide area damping controller using PDCI modulation and real-time PMU feedback," *2016 IEEE Power and Energy Society General Meeting (PESGM)*, 2016, pp. 1-5, doi: 10.1109/PESGM.2016.7741594.

[16] S. Yu, T. K. Chau, T. Fernando, A. V. Savkin and H. H. -C. Iu, "Novel Quasi-Decentralized SMC-Based Frequency and Voltage Stability Enhancement Strategies Using Valve Position Control and FACTS Device," in *IEEE Access,* vol. 5, pp. 946-955, 2017, doi: 10.1109/ACCESS.2016.2622709.

[17] Y. Wan, M. A. A. Murad, M. Liu and F. Milano, "Voltage Frequency Control Using SVC Devices Coupled With Voltage Dependent Loads," in *IEEE Transactions on Power Systems,* vol. 34, no. 2, pp. 1589-1597, March 2019, doi: 10.1109/TPWRS.2018.2878963.

[18] M. A. A. Murad, G. Tzounas, M. Liu and F. Milano, "Frequency Control Through Voltage Regulation of Power System Using SVC Devices," *2019 IEEE Power & Energy Society General Meeting (PESGM),* 2019, pp. 1-5, doi: 10.1109/PESGM40551.2019.8973807.

[19] R. M. Mathur; R. K. Varma, "Emerging FACTS Controllers," in *Thyristor-Based FACTS Controllers for Electrical Transmission Systems,* IEEE, 2002, pp.413-461, doi: 10.1109/9780470546680.ch10.

[20] A. Hewitt and T. Ahfock, "Harmonic injection due to negative phase sequence correction in static VAr compensators," *2015 Australasian Universities Power Engineering Conference (AUPEC),* 2015, pp. 1-5, doi: 10.1109/AUPEC.2015.7324844.

[21] Y. Ma, L. Cao, X. Zhou and Z. Gao, "The discussion on static synchronous compensator technology," *2016 IEEE International Conference on Mechatronics and Automation,* 2016, pp. 106-111, doi: 10.1109/ICMA.2016.7558543.

[22] T. Tayyebifar, M. Shaker and M. Aghababaie, "Performance comparison of STATCOM versus SVC to improve reactive power control in wind power based DFIG under short circuit fault," *2014 Ninth International Conference on Ecological Vehicles and Renewable Energies (EVER),* 2014, pp. 1-7, doi: 10.1109/EVER.2014.6844049.

[23] C. Li et al., "Enhancement of power system small-signal stability by coordinated damping control of multiple FACTS devices," *13th IET International Conference on AC and DC Power Transmission (ACDC 2017),* 2017, pp. 1-6, doi: 10.1049/cp.2017.0007.

[24] B. Kirby, "Frequency Regulation Basics and Trends," Oak Ridge National Laboratory, Oak Ridge, Tennessee 37831-6283, Dec. 2004 [Online]. Available: https://info.ornl.gov/sites/publications/Files/Pub57475.pdf. [Accessed: Apr. 23, 2022]

[25] P. Tumino, "Frequency Control in a Power System," *EE Power,* Oct. 15, 2020. [Online]. Available: https://eepower.com/technical-articles/frequency-control-in-a-power-system/#. [Accessed: Apr. 23, 2022]

[26] A. von Meier, "System Performance," in *Electric Power Systems: A Conceptual Introduction*, IEEE, 2006, pp.229-258, doi: 10.1002/0470036427.ch8.

[27] G. Delille, L. Capely, D. Souque and C. Ferrouillat, "Experimental validation of a novel approach to stabilize power system frequency by taking advantage of Load Voltage Sensitivity," *2015 IEEE Eindhoven PowerTech,* 2015, pp. 1-6, doi: 10.1109/PTC.2015.7232697.

[28] M. Hojabri et al., "A Comprehensive Survey of Phasor Measurement Unit Applications in Distribution Systems," MDPI, 29 November 2019. Accessed: 1 Jan 2022. Available: https://www.mdpi.com/1996-1073/12/23/4552/pdf

[29] R. M. Mathur; R. K. Varma, "Introduction," in *Thyristor-Based FACTS Controllers for Electrical Transmission Systems,* IEEE, 2002, pp.221-276, doi: 10.1109/9780470546680.ch6.

[30] R. M. Mathur; R. K. Varma, "Principles of Conventional ReactivePower Compensators," in *Thyristor-Based FACTS Controllers for Electrical Transmission Systems* , IEEE, 2002, pp.40-92, doi: 10.1109/9780470546680.ch3.

[31] R. M. Mathur; R. K. Varma, "SVC Applications," in *Thyristor-Based FACTS Controllers for Electrical Transmission Systems,* IEEE, 2002, pp.221-276, doi: 10.1109/9780470546680.ch6.

[32] "Phasor Measurement Unit (PMU) Implementation and Applications," Electronic Power Research Institute (EPRI), Palo Alto, CA, 1015511, Oct. 2007 [Online]. Available: https://www.epri.com/research/products/1015511

[33] J. O'Brien, Frequency-Domain Control Design for High-Performance Systems, London: The Institution of Engineering and Technology, 1994.

[34] A. Tangirala, Principles of System Identification, Florida: CRC Press Taylor & Francis Group, 2015.

[35] B. J. Lurie, Feedback Maximization, Dedham, MA: Artech House, 1986.

[36] M. EL-Shimy, M. A. L. Badr and O. M. Rassem, "Impact of large scale wind power on power system stability," *2008 12th International Middle-East Power System Conference,* 2008, pp. 630-636, doi: 10.1109/MEPCON.2008.4562365.

[37] A. Shrestha and F. Gonzalez-Longatt, "Frequency Stability Issues and Research Opportunities in Converter Dominated Power System," *Energies,* vol. 14, no. 14, p. 4184, Jul. 2021, doi: 10.3390/en14144184. [Online]. Available: https://www.mdpi.com/1996-1073/14/14/4184. [Accessed: Apr. 16, 2022]